의학석사 학위논문

Population pharmacokinetic analysis of GX-E2, a novel erythropoiesis stimulating agent, in healthy male subjects

새로운 적혈구 생성 촉진제인 GX-E2의 집단 약동학 분석

2018 년 2 월

서울대학교 대학원

의과학과 의과학전공

윤 수 민

Population pharmacokinetic analysis of GX-E2, a novel erythropoiesis stimulating agent, in healthy male subjects

지도 교수 유 경 상

이 논문을 의학석사 학위논문으로 제출함

2017년 10월

서울대학교 대학원

의과학과 의과학전공

윤 수 민

윤수민의 의학석사 학위논문을 인준함

2018년 1월

위 원 장 _____ (인)

부위원장 _____ (인)

위 원 _____ (인)

ABSTRACT

Population pharmacokinetic analysis of GX-E2, a novel erythropoiesis stimulating agent, in healthy male subjects

Sumin Yoon

Major in Biomedical Sciences,

Department of Biomedical Sciences,

The Graduate School

Seoul National University

Introduction: GX-E2 is a novel erythropoiesis stimulating agent which is human erythropoietin (EPO) fused with Fc region of the antibody. The pharmacokinetic (PK)/pharmacodynamic (PD) properties following a single intravenous (IV) and subcutaneous (SC) injection of GX-E2 have been revealed by the noncompartmental analysis of preclinical and clinical study. The SC injection of GX-E2 presented the extended mean residence time and duration of action than currently marketed EPO.

The objective of this study was to characterize the PK properties following a sin-gle IV and SC injection of GX-E2 by developing population PK models.

Methods: For the model development, data were pooled from two phase I clinical trials. Two different approaches were applied for describing the disposition of GX-E2: Simple disposition model in which describes the model with Michaelis-Menten enzyme kinetics were tested. Target-mediated drug disposition (TMDD) model was tested for mechanistic understanding of PK properties. Each model was numerically and graphically diagnosed to select the final model. Visual predictive check was per-formed to validate the predictive performance of the final model.

Results: A total of 1084 serum GX-E2 concentrations were obtained from 72 sub-jects. The PK properties of GX-E2 were well described by the 2-compartment model with first-order absorption. Both Michaelis-Menten enzyme kinetic model and TMDD model could adequately explain the characteristic PK profiles of GX-E2. An acceptable predictive performance of each final model was validated by the visual predictive check. Approximately 50 – 70% of the SC injected dose was predicted to be absorbed into the systemic circulation with the first-order absorption constant of 0.003 h^{-1}. From the estimated clearances of free-form and bound form, majority of injected GX-E2 are predicted to be eliminated as a bound form.

Conclusion: This study first described the PK of GX-E2 by developing population PK models. Both simple disposition model and TMDD model were fitted well with the observed data, how-ever, TMDD model had advantage in reflecting mechanistic

aspects of drug. Further assessments of absorption mechanism and inclusion of PD factors in current model will enable to assess the further in-depth understanding of GX-E2 PK profile.

Keywords: Population pharmacokinetics; Michaelis-Menten; target-mediated drug disposition; NONMEM; GX-E2; erythropoietin stimulating agent

Student number: 2015-23241

TABLE OF CONTENTS

LIST OF TABLES

LIST OF FIGURES

LIST OF ABBREVIATIONS AND SYMBOLS

PK	Pharmacokinetic
PD	Pharmacodynamic
EPO	Erythropoietin
rhuEPO	Recombinant human erythropoietin
IV	Intravenous
SC	Subcutaneous
NONMEM	Nonlinear mixed effect modeling
LLOQ	Lower limits of quantification
IIV	Inter-individual variability
TMDD	Target-mediated drug disposition
VPC	Visual predictive check
RSE	Relative standard error
C_{max}	Maximum observed concentration
AUC_{last}	Area under the curve from the time of dosing to the last measurable concentration
$AUC_{0\text{-}24h}$	Area under the curve from the time of dosing to the 24-hour pose-dose
AUC_{inf}	Area under the curve from the time of dosing extrapolated to infinity, based on the last observed concentration

λ_z	The estimated first-order terminal elimination rate constant
V_d	Volume of distribution
CL/F	Total body clearance
MRT	Mean residence time
IPRED	Individual predicted value
OFV	Objective function value
CWRES	Conditional weighted residuals
V_m	Maximum rate of elimination
K_m	Serum GX-E2 concentration giving 50% of the maximum rate
CL_A	Clearance of the free drug
CL_B	Clearance of the drug and target receptor complex
RB	Input rate of target receptor
K_D	Equilibrium dissociation constant
k_a	Absorption rate constant

INTRODUCTION

Erythropoietin (EPO) is a glycoprotein hormone which promotes and regulates the red blood cell production. EPO is mainly produced in the kidney and stimulates erythropoiesis by binding to the EPO receptor on the surface of erythroid progenitor cell in the bone marrow. (1) Because EPO is insufficiently produced in patient with chronic kidney disease, anemia is a common complication of chronic kidney disease. Therefore, initiating an erythropoiesis-stimulating agent such as recombinant human EPO (rhuEPO) is recommended for patients with anemia in chronic kidney disease after addressing all correctable causes of anemia including iron deficiency and inflammatory states. (2)

Using recombinant DNA technology in cell culture, EPO could be produced *ex vivo.* It enabled the massive production of recombinant human EPO (rhuEPO). Number of rhuEPO such as epoetin alfa, epoetin beta and darbepoetin alfa were developed with a variety of glycosylation pattern. These rhuEPO formulations have been used in clinical settings for over 30 years for the treatment of anemia.

Unlike the currently marketed rhuEPO, GX-E2 (Genexine, Inc., Seongnam-si, Republic of Korea; formerly also known as GC1113) is a novel erythropoietin-stimulating agent, which fused the fragment crystallizable (Fc) protein of antibody with EPO, in anticipation of longer acting time. (3) In general, the Fc region of the antibody binds to the Fc-γ receptor of the endothelial cell membrane surface and delays the degradation of the antibody. (4) Thus, the Fc-fused therapeutic protein is expected to have an increased half-life and prolonged duration of action. (5, 6) GX-E2 is a long-acting erythropoietin stimulating agent containing two EPO molecules

fused with the hybrid Fc region of human IgD and IgG4. GX-E2 showed comparable or longer serum terminal half-life than that of darbepoetin alfa in preclinical studies. (3) Furthermore, subcutaneous (SC) GX-E2 presented extended duration of increased reticulocyte counts than that of darbepoetin alfa in both preclinical and clinical studies, while intravenously (IV) administered GX-E2 presented comparable duration with that of darbepoetin alfa. (3, 7)

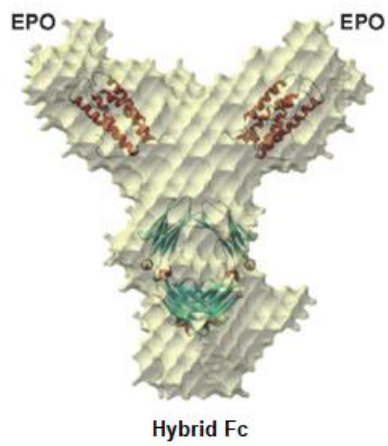

Figure 1. The protein structure of GX-E2
(adopted from Im et al., 2011)

Nowadays, thorough assessments of the drug properties are essential at the early stages of the new drug development. Pharmacokinetic (PK) assessment plays a pivotal role in early clinical phase of the drug development. (8) In the traditional approach of PK assessment, individual PK parameter values are generally obtained by noncompartmental analysis with sufficient number of samplings first. Then, population parameters are obtained by calculating the mean of individual parameter values without statistical concepts. The population PK approach using nonlinear

mixed effect modeling was established by Sheiner and Beal in 1970s. (9) The typical population PK parameters with inter-individual variability (IIV) and individual PK parameters with residual (inter-occasional) variability could be estimated with the population approach proposed by Sheiner and Beal. The original purpose of the population PK approach was to analyze the sparse data which was obtained routinely from the therapeutic drug monitoring process. (10) Population PK analysis using nonlinear mixed effect modeling approach have the number of advantages for the quantitative understanding of PK. First, it enables to obtain the population parameter values with individual parameter values with distributions of each variability. Besides, not only dense data but also sparse or unbalanced data can be pooled and integrated in a single model. It enabled the analysis of PK and/or PD from special populations such as pediatric and elderly populations that have difficulties in dense sampling. (11) Lastly, significant covariates which can be sources of inter-individual variability can be identified. (12) Consequently, population PK modeling has a considerable role by supporting as a base for the pivotal regulatory approval decisions.

PK analyses with population PK models have been reported for rhuEPO including epoetin alfa and darbepoetin alfa (13-17). As observed in other therapeutic protein, the nonlinear disposition of rhuEPO has been consistently observed. The receptor-mediated endocytosis caused by the binding of drug to its receptor and lysosomal degradation are reported for the cause of the characteristic PK properties (18). To deal with this nonlinear properties, two approaches are commonly incorporated. One is a saturable elimination pathway which is parameterized by Michaelis-Menten constant K_m and V_{max} and the other is a more mechanistic model that is

used to describe the target-mediated drug disposition (TMDD). (19) The TMDD corresponds to a case where a drug is bound with high affinity to its target, and this interaction affects the PK properties of the drug in a dose-dependent manner. TMDD uses saturable, high affinity receptor binding mechanism as a primary mechanism of nonlinear pharmacokinetics of EPO. Another key assumption of the model is that receptor-mediate endocytosis contributes to EPO elimination. (20)

In cases of other rhuEPO, population PK/PD models have been developed without or with the concepts of TMDD. (21, 22) However, a population analysis of GX-E2 has not been conducted yet. Hence, the current study developed and compared two population PK models – one with saturable elimination pathway and the other with TMDD – to support the description of PK following a single IV or SC injection of GX-E2.

METHODS

Studies and subjects

The GX-E2 data from two phase I clinical studies were included for the population PK analysis. In the first study (study 1), the PK and PD characteristics of a single IV or SC dose of GX-E2 were assessed (Clinicaltrials.gov identifier: NCT01363934). The dose groups for each route of administration were as follows: 0.3, 1, 3, or 5 μg/kg IV GX-E2 and 1, 3, 5, or 8 μg/kg SC GX-E2. For the active control, IV and SC doses of Nesp® (darbepoietin alfa) 30 μg/kg were administered. Ten subjects were assigned to each dose group; eight subjects received the test drug while two subjects received the placebo. The blood samplings for the PK and PD analysis were conducted before the drug administration and for up to 672 hours after the drug administration (PK blood sampling: 0.25, 0.5, 1, 2, 3, 4, 6, 8, 12, 24, 36, 48, 60, 72, 96, 120, 168, 240, 336, 504, and 672 hours; PD blood sampling: 4, 8, 12, 24, 48, 60, 72, 96, 120, 168, 240, 336, 504, and 672 hours). The PK blood samples were centrifuged at 4℃, 3,000 rpm for 10 minutes. The separated sera were stored under -70 ℃ until the bioanalysis.

In the second study (study 2), the PK and PD characteristics of a single 8 μg/kg IV dose of GX-E2 were assessed. (Clinicaltrials.gov identifier: NCT02291991) As in study 1, ten subjects were assigned to each dose group; eight subjects received the test drug while two subjects received the placebo. The blood sampling time points for the PK and PD analyses were same as the study 1. The collected PK samples went through same pretreatment procedures ahead of the bioanalysis as those of the study 1.

Data from subjects who were administered GX-E2 were utilized for the model development. That is, data from subjects who were administered NESP® in study 1 or placebo in study 2 were excluded from the analysis.

Both studies were conducted at the Clinical Trials Center of Seoul National University Hospital (SNUH), Seoul, Republic of Korea. The study protocols and informed consent forms were approved by the Institutional Review Board of the SNUH. All subjects participated in the study voluntarily after providing their written informed consent. These studies were performed in compliance with the Declaration of Helsinki, and all study procedures were done in accordance with the Guideline for Good Clinical Practice of International Conference on Harmonization. (23, 24)

Table 1. Summary of pooled clinical trials

	Study 1	Study 2
Number of subjects	80	10
Subject characteristics	Healthy male subjects	Healthy male subjects
Study characteristics	First-in-human, PK/PD study	First-in-human, PK/PD study
Drug administration (GX-E2)	Single dose; (IV) 0.3, 1, 3 and 5 μg/kg (SC) 1, 3, 5 and 8 μg/kg	Single dose; (IV) 8 μg/kg
PK sampling time	pre-dose, 0.25, 0.5, 1, 2, 3, 4, 6, 8, 12, 24, 36, 48, 60, 72, 96, 120, 168, 240, 336, 504, and 672 hours post-dose	pre-dose, 0.25, 0.5, 1, 2, 3, 4, 6, 8, 12, 24, 36, 48, 60, 72, 96, 120, 168, 240, 336, 504, and 672 hours post-dose
Lower limit of quantification	(IV) 0.3, 1, 3, 5, 8 μg/kg: 1.56 ng/mL (SC) 1, 3, 5 μg/kg: 156.25 pg/mL	78.125 pg/mL
ClinicalTrials.gov identifier	NCT1363934	NCT02291991

Abbreviations: PK, pharmacokinetics; PD, pharmacodynamics; IV, intravenous; SC, subcutaneous.

Bioanalytical methods

The serum isolated from each blood sample was analyzed for GX-E2 concentrations by the Clinical Pharmacology Bioanalytical Research Team, Department of Clinical Pharmacology and Therapeutics, Seoul National University College of Medicine and Hospital. In study 1, the serum GX-E2 concentrations were determined by enzyme-linked immunosorbent assay (ELISA) with the human EPO Immunoassay kit (R&D Systems Inc., Minneapolis, MN, USA) using the microplate reader SpectraMax M2 (Molecular Devices, Sunnyvale, CA, USA). The inter-assay accuracy and precision of the quality control sample data were 91.03 – 114.9% and <6.641%, respectively. In study 2, the serum EPO concentrations were determined with the human EPO immunoassay kit using the SpectraMax 190 (Molecular Devices, Sunnyvale, CA, USA). The inter-assay accuracy and precision were 91.5 – 94.4%, and <6.218%, respectively.

The lower limits of quantification (LLOQ) of the serum EPO differed by the dose groups and studies. In study 1, the LLOQ for the IV group was 1.56 ng/mL, while the LLOQ was 156.25 and 78.13 pg/mL for the 1, 3, and 5 μg/kg doses and 8 μg/kg dose for the SC group, respectively. In study 2, the LLOQ was 78.13 pg/mL (8 μg/kg dose for the IV group).

Population pharmacokinetic analysis

Parameter estimation method

For the population PK analysis, nonlinear mixed effect modeling was performed using the NONMEM software version 7.4 (ICON Development Solutions, Ellicott City, MD, USA) with the Perl-speaks-NONMEM version 4.7.0. The Pirana software version 2.9.6 (Pirana Software & Consulting BV) was utilized as a workbench for NONMEM. (25) R version 3.4.2 (R Foundation for Statistical Computing, Vienna, Austria) was used for the data processing including graphical analysis. The expectation-maximization (EM) method aided by the MU-referencing were used for the parameter estimation. (26, 27) The EM method has reported to have an advantage in relatively fast estimation runtime for the complex models and the rate of successful convergence. (28) In addition, MU-referencing enables the effective application of method. (29)

Simple disposition model

To describe the disposition of serum EPO following the IV or SC injection of GX-E2, one and two compartment base structural models with saturable elimination pathway were developed and compared (**Table 2**).

Saturable elimination pathway was described with Michaelis-Menten enzyme kinetics, which parameterize the model by the maximum rate of elimination (V_m) and the serum EPO concentration giving 50% of the maximum rate (K_m). (30) The initial estimate of each PK parameter was determined by referring the non-compartmental analysis results and the previously reported population PK/PD models for rhuEPO. (13, 15, 21, 31)

Table 2. Description of tested models (simple disposition model)

Model Description	Subroutines	Pharmacokinetic Parameters
1-compartment model with nonlinear elimination	ADVAN13 TRANS1	$V_{C,}$ $V_{m,}$ $K_{m,}$ $k_{a,}$ F
2-compartment model with nonlinear elimination	ADVAN13 TRANS1	V_C, V_P, V_m, K_m, Q, $k_{a,}$ F

Abbreviations: V_C, volume of central compartment; CL, total clearance; k_a, absorption rate constant V_m, maximum rate of elimination; K_m, the serum EPO concentration giving 50% of the maximum rate; V_P, volume of peripheral compartment; Q, intercompartmental flow rate.

Assuming that PK parameters follow the log-normal distribution, an exponential error model was used to describe the IIV of each PK parameter:

$$P_i = \theta_P \cdot \exp(\eta_i) \quad (1)$$

where P_i denotes the individual estimated value of parameter of i^{th} subject, θ_p is the typical value of parameter (population value) and η_i is IIV of parameter of i^{th} subject. η_i is assumed to follow a normal distribution with a mean of zero and a variance of ω_i^2 ($\eta_i \sim N(0, \omega_i^2)$).

A combined additive and proportional error model was used to estimate the residual variability. (32)

$$Y_{ij} = IPRED_{ij} + \sqrt{(\varepsilon_{PROP,ij} \times IPRED_{ij})^2 + \varepsilon_{ADD,ij}^2} \quad (2)$$

where Y_{ij} is a observed value for j^{th} occasion of i^{th} subject, $IPRED_{ij}$ is the corresponding individual predicted value, $\varepsilon_{prop,ij}$ is proportional residual error and $\varepsilon_{add,ij}$ is an additive residual error for the corresponding occasion and subject. ε_{ij} is assumed to follow a normal distribution with a mean of zero and a variance of σ_{ij}^2 ($\varepsilon_{ij} \sim N(0, \sigma_{ij}^2)$).

Target-mediated drug disposition model

A target-mediated disposition (TMDD) model was developed together to include the effect of the EPO and EPO receptor binding and receptor-mediated endocytosis on PK properties. The two-compartment, target-on-tissue TMDD model was developed by referring to the TMDD PK model proposed by Mager and Jusko. (33) The schematic illustration of the basic TMDD model structure is presented in **Figure 2**.

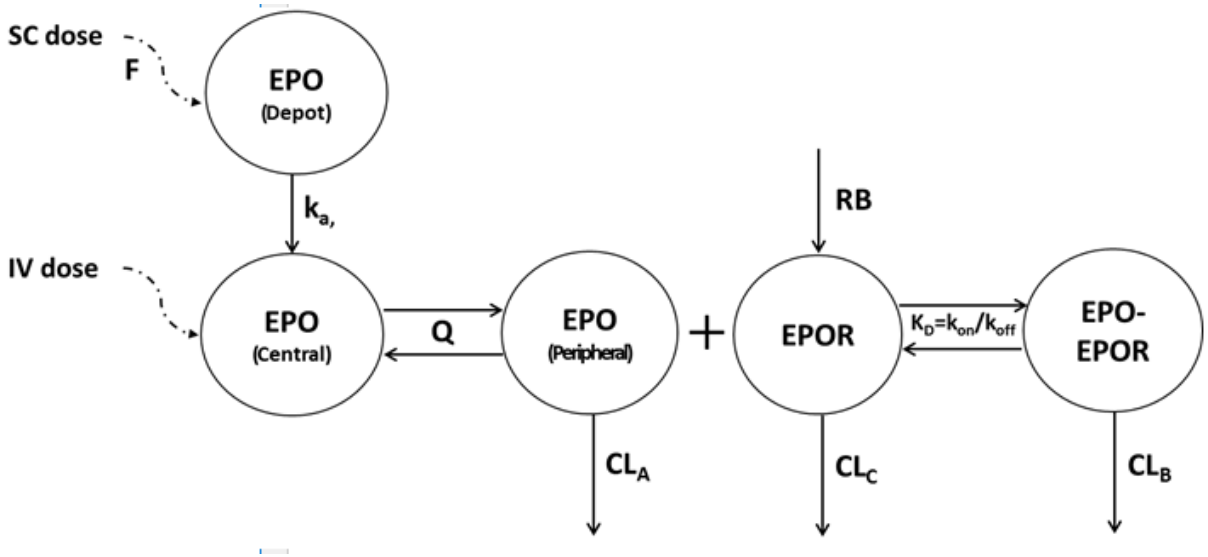

Figure 2. The schematic diagram of the target-mediated drug disposition model for a single IV or SC administration of GX-E2.

Abbreviations: SC, subcutaneous; IV, intravenous; F, bioavailability; k_a, absorption rate constant; Q, intercompartmental flow rate; EPO, erythropoietin; EPOR, erythropoietin receptor; CL_A, clearance of free EPO in the peripheral compartment; CL_B, clearance of EPO-EPO receptor complex in the peripheral compartment; CL_C, clearance of the EPO receptor; RB, input rate of binding target; K_D, equilibrium dissociation constant

In this model, the faith of EPO in systemic circulation is determined between two pathways: 1) eliminated from the central compartment (CL_A) as a free EPO form or 2) bound to the EPO receptor of the progenitor cells in the bone marrow and degraded as a EPO-EPO receptor complex form (CL_B). When establishing mass-balance equations for each compartment, two assumptions were made. When EPO binds to the EPO receptor with high affinity, it has been reported that the internalization of the target-receptor complex occurs as free EPO receptor is degenerated. (34) Thus, the internalization rate of the EPO-EPO receptor complex (CL_B) is assumed to be same as the degeneration rate of the target (CL_C) (35, 36) In addition, the K_D is assumed same as the k_{off}/k_{on}, in which k_{off} is the dissociation constant, and k_{on} is the binding constant. In an essence, the mass-balance equations for free EPO of the central and peripheral compartments (A and A_P, respectively) are as follows:

$$\frac{\mathrm{dA}}{\mathrm{dt}} = (Input) - \frac{CL_A}{V_C} \cdot A - \frac{Q}{V_C} \cdot A + \frac{Q}{V_P} \cdot A_P \quad (3)$$

$$\frac{\mathrm{d}A_P}{\mathrm{dt}} = -\frac{CL_B}{V_P} \cdot CPLX + \frac{Q}{V_C} \cdot A - \frac{Q}{V_P} \cdot A_P \quad (4)$$

, where CL_A is the clearance of the free EPO in the central compartment; V_c is the volume of the central compartment; V_P is the volume of the peripheral compartment; Q is the intercompartmental flow rate; CPLX is the amount of the EPO-EPO receptor complex in the peripheral compartment and CL_B is the clearance of the EPO-EPO receptor complex in the peripheral compartment, which was assumed to be the same as the CL_C (the degeneration rate of the free EPO receptor) in this

study.

The amounts of total EPO (TA_P), total EPO receptor (TB_P) and EPO-EPO receptor complex (CPLX) in the peripheral compartment are described with the following equations:

$$TA_p = A_P + CPLX \tag{5}$$

$$TB_P = \frac{V_P \cdot RB}{CL_B} \tag{6}$$

$$\mathrm{CPLX} = \frac{1}{2} \cdot [(K_D \cdot V_P + TA_P + TB_P) - \sqrt{(K_D \cdot V_P + TA_P + TB_P)^2 - 4 \cdot TA_P \cdot TB_P} \tag{7}$$

, where A_P is the amount of EPO in the peripheral compartment; RB is the input rate of binding target, K_D is an equilibrium dissociation constant and V_P is the volume of the peripheral compartment.

The derivation of the equation describing the amount of EPO-EPO receptor complex (eq. (7)) was previously described in the previously published literature. (35)

The initial values were selected based on the previous literature describing the PK of EPO and the preclinical study results of GX-E2. (3, 13, 15, 21, 31) The K_D, the equilibrium dissociation constant, was fixed as 0.2 nM based on its *in vitro* study results with GX-E2 (J. Woo, personal communication, April 27, 2017). Variability model for TMDD was developed in the same way with the simple disposition model.

Model selection

Both numerical and graphical methods were applied when judging the model improvement. For the numerical methods, objective function value (OFV, -2log likelihood), the results of the likelihood ratio test, and Akaike's information criterion (AIC) value were calculated for each model by following formulae:

$$\mathrm{OFV} = -2\log(\mathrm{L}) = \mathrm{nlog}(2\pi) + \sum_{i=1}^{n}(\log(\sigma_i^2) + \frac{\left(Y_i - \hat{Y}_i\right)^2}{\sigma_i^2}) \quad (8)$$

$$\mathrm{AIC} = \mathrm{OFV} + 2 \cdot \text{number of parameters} \quad (9)$$

,where L is likelihood, n is the number of observations, Y_i is the observed value of i[th] subject, $\hat{Y}_i$ is the predicted value of i[th] subject, and σ_i^2 is the variance.

OFV, the results of the likelihood ratio test, was used for comparing rival nested models. By increasing the likelihood ratio (L), the OFV is minimized. As $\mathrm{nlog}(2\pi)$ is a constant term, maximizing the likelihood ratio is achieved by maximizing the $\sum_{i=1}^{n}(\log(\sigma_i^2) + \frac{(Y_i-\hat{Y}_i)^2}{\sigma_i^2})$ term, so called extended least square (ELS). Since the likelihood ratio ($-2\log(\frac{L_2}{L_1})$) has been reported to follow the χ-distribution, a reduction of the minimum OFV more than 3.84 was considered to have reached statistical significance at $P < 0.05$ for the addition of one degree of freedom (fixed effect). (37)

For the graphical method, a visual-inspected improvement of goodness-of-fit plots with individual plots was assessed. The goodness-of-fit plots included individual predictions *versus* observed data, population predictions *versus* observed data, population predictions *versus* conditional weighted residuals (CWRES) and

time *versus* CWRES. Furthermore, time *versus* individual predictions plotted with individual observed data was assessed. Lastly, the physiological plausibility of each parameter estimate was considered.

Covariate selection

Covariate analysis was performed in order to identify additional variables which could explain the variabilities presented in the parameter estimates from the final models. Tested covariates included age, height, weight, reticulocyte, hemoglobin and reticulocyte hemoglobin content. The relationship of each covariate and IIV for each parameter were investigated using visual inspection. Visual inspection was performed with Xpose toolkit version 4.3.5 within R version 3.4.2 (R Foundation for Statistical Computing, Vienna, Austria). Covariates showing a trend in the scatter plot (covariates *versus* IIV of parameter) were applied to the model with a stepwise manner with forward inclusion and backward deletion.

Model validation

To assess the predictive performance of the final model, an internal model validation was performed using prediction-corrected visual predictive check (pcVPC). The traditional VPC without prediction and/or variability normalization may fail in an adequate predictive performance assessment of the model when the expected value or expected variability in observations within a same bin differs due to variations in predictors such as sampling time and administered dose. Hence, in the pcVPC, both the observed and predicted values are normalized for the typical model predictions. (38, 39)

The pcVPC was implemented in the NONMEM software version 7.4 (ICON Development, Ellicott City, MD, USA) with the Perl-speaks-NONMEM toolkit version 4.6.0 and Xpose toolkit version 4.3.5. A total of 1000 datasets of concentrations by each timepoint were simulated using the final model. Then, 95% confidence intervals (CIs) for 5^{th}, 50^{th} (median) and 95^{th} percentiles of the simulated values were obtained and shown as area. The model was considered to have a satisfactory prediction performance if the observed values were within shaded CI area.

RESULTS

Study populations

A total of 1084 serum EPO concentrations from 72 healthy subjects were available for the development of the population PK model (64 subjects and 8 subjects for study 1 and study 2, respectively). The mean ± standard deviation values of age, height, weight and BMI of the pooled subjects were 26.4 ± 4.7 years, 175.2 ± 5.0 cm, 70.2 ± 6.0 kg and 22.8 kg/m^2, respectively. Demographic information of the subjects is summarized by the study in **Table 3**.

Table 3. Baseline demographic characteristics of pooled subjects by the study.

	Study 1	Study 2	Pooled subjects
Number of the subjects*	64	8	72
Age (years)	25.91 ± 4.61	30.8 ± 2.8	26.4 ± 4.7
Height (cm)	175.78 ± 4.85	173.1 ± 4.7	175.2 ± 5.0
Weight (kg)	70.17 ± 6.24	70.5 ± 3.5	70.2 ± 6.0
Body Mass Index (kg/m^2)	22.72 ± 1.91	23.6 ± 1.9	22.8 ± 1.9
Body Surface Area (m^2)**	1.85 ± 0.09	1.8 ± 0.1	1.8 ± 0.1
Baseline			
Reticulocyte count (%)	1.0 ± 0.3	1.5 ± 0.2	1.0 ± 0.4
Hemoglobin (g/dL)	14.7 ± 0.8	15.1 ± 0.7	14.8 ± 0.8

Values are presented as mean ± standard deviation.

*Subjects who took the NESP® in study 1 or placebo in study 2 were excluded.

**Body surface area was calculated by Mosteller formula ($=\sqrt{\frac{Weight\ (cm) \times Height\ (cm)}{3600}}$).

Exploratory data analysis

The mean concentration-time profiles of GX-E2 following a single IV or SC injection are provided in **Figure 3**. PK parameters obtained from noncompartmental analysis are provided in the Appendices. Following the IV administration, a distinct nonlinear disposition profile was observed. CL/F presented decreasing tendency as dose of GX-E2 increases. The IV injected GX-E2 are expected to reside in the body for 1.99 (0.3 µg/kg), 3.87 (1 µg/kg), 7.98 (3 µg/kg), 10.51 (5 µg/kg), and 22.29 h (8 µg/kg) postdose.

When administered subcutaneously, GX-E2 reached its maximum concentration at 6 to 36 hours after the injection and presented prolonged peak, indicating slow absorption process. CL/F presented increasing tendency as dose of GX-E2 increases. The MRT following SC injection highly exceeded when compared with those following corresponding dose injected intravenously. GX-E2 are expected to reside in the body for 227.83 (1 µg/kg), 218.73 (3 µg/kg), 210.52 (5 µg/kg) and 199.78 (7 µg/kg) hour after the SC injection.

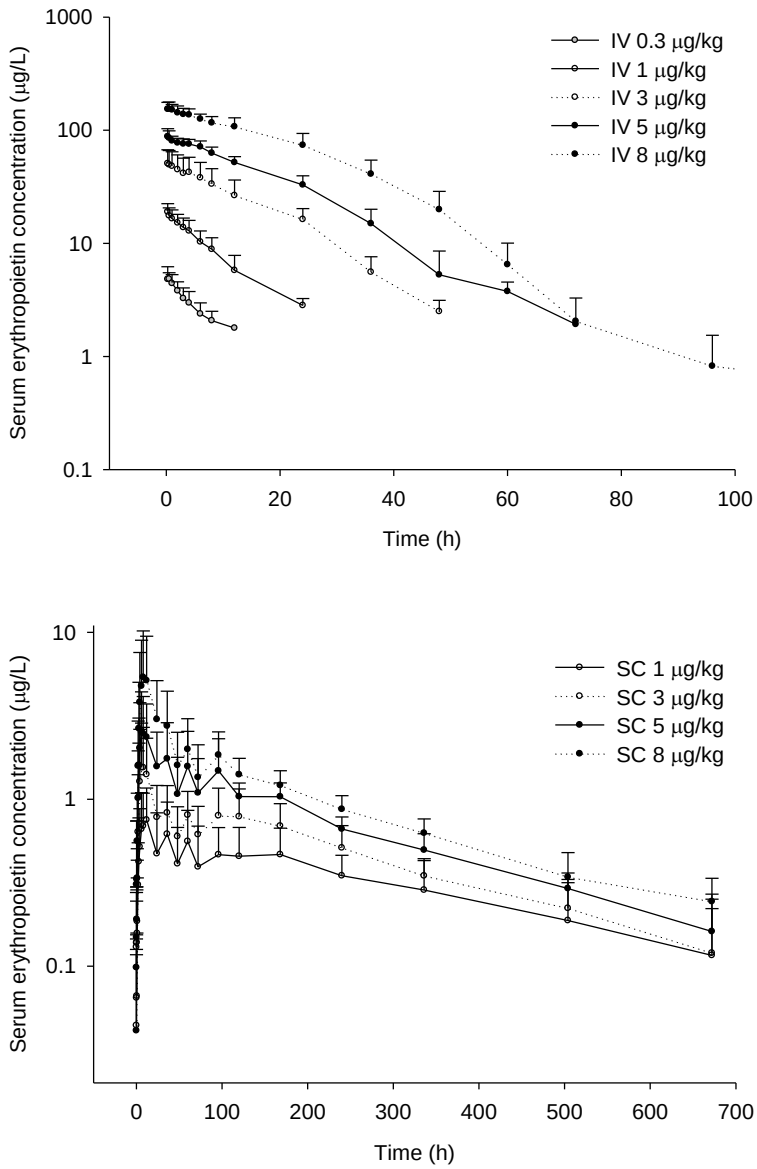

Figure 3. Serum GX-E2 concentration-time profile following a single IV (left) or SC (right) administration of GX-E2 in healthy male volunteers (semi-logarithmic scale)

Abbreviations: IV, intravenous; SC, subcutaneous

Population pharmacokinetic analysis

Simple disposition model

When the nonlinear disposition of GX-E2 was described with saturable elimination pathway, two-compartment model explained the PK properties better than one-compartment model. (ΔOFV=193.674 and ΔAIC=107.674). The mass-balance equations for central and peripheral compartment of final PK model were as follows:

$$\frac{dA}{dt} = (Input) - \frac{Q}{V_C} \cdot A + \frac{Q}{V_P} \cdot A_P - \frac{V_m \cdot C}{K_m + C} \quad (10)$$

$$\frac{dA_p}{dt} = \frac{Q}{V_C} \cdot A - \frac{Q}{V_P} \cdot A_P \quad (11)$$

where A is the amount of EPO in serum (central compartment), A_p is the amount of EPO in peripheral compartment, V_C is s the volume of the central compartment, V_p is s the volume of the peripheral compartment, Q is the intercompartmental flow rate, V_m is the maximum rate of elimination and K_m is the serum EPO concentration giving 50% of the maximum rate.

C, the EPO concentration of central compartment was parameterized by A and V_C as follows:

$$C = \frac{A}{V_C} \quad (12)$$

where A is the amount of EPO in serum (central compartment) and V_C is the volume of the central compartment.

Visual inspections of IIV for parameter and potential covariate (age, height, weight, reticulocyte, hemoglobin and reticulocyte hemoglobin content) presented that IIV generally distributed around zero (Appendix 2). Thus, covariates were not included in the final model.

From the final simple disposition model, the V_C and V_P were estimated 4.05 L and 84 L, respectively. The V_m and K_m values were estimated at 127 pmol/h and 408 pmol/L, respectively. The parameters regarding absorption process, k_a and F were estimated at 0.0152 h^{-1} and 0.529 respectively. The IIV as ETA was allowed to every PK parameters, except V_m. Other estimated values for PK parameter and its variability obtained from the final model are presented in **Table 4.**

Table 4. Parameter estimates and inter-individual variability for the population PK model of GX-E2 (simple disposition model)

Parameter	Definition	Population estimate (%RSE)	Inter-individual variability*
Pharmacokinetic parameter			
V_C (L)	Volume of central compartment	4.05 (12)	5.7
V_P (L)	Volume of peripheral compartment	84 (15)	48.8
Q (L/h)	Intercompartmental flow rate	0.221 (25)	180.3
V_m (pmol/h)	Maximum rate of elimination	127 (4)**	-
K_m (pmol/L)	Serum GX-E2 concentration giving 50% of the maximum rate	408 (3)	1.9
k_a (h^{-1})	Absorption rate constant (first-order)	0.0152 (21)	85.3
F	Bioavailability	0.529 (12)	50.5
Residual variability			
Proportional error (%)		31.7	-
Additional error (pmol/L)		0.001**	-
Running information			
Objective Function Value		5858.879	
Akaike Information Criteria		6054.872	
Elapsed estimation time (sec)		1032.91	

*Data is presented as percent (%).

**Fixed

Abbreviations: RSE, relative standard error

Figure 4 presents the goodness-of-fit plots of the final model. The scatter plots of the observed *versus* population predicted concentrations and observed *versus* individual predicted concentrations were distributed symmetrically around the line of unity. The CWRES were randomly distributed around zero and mostly were within the range of -2 to 2. Individual plots present that most observations were explained by the population PK model (**Figure 5**).

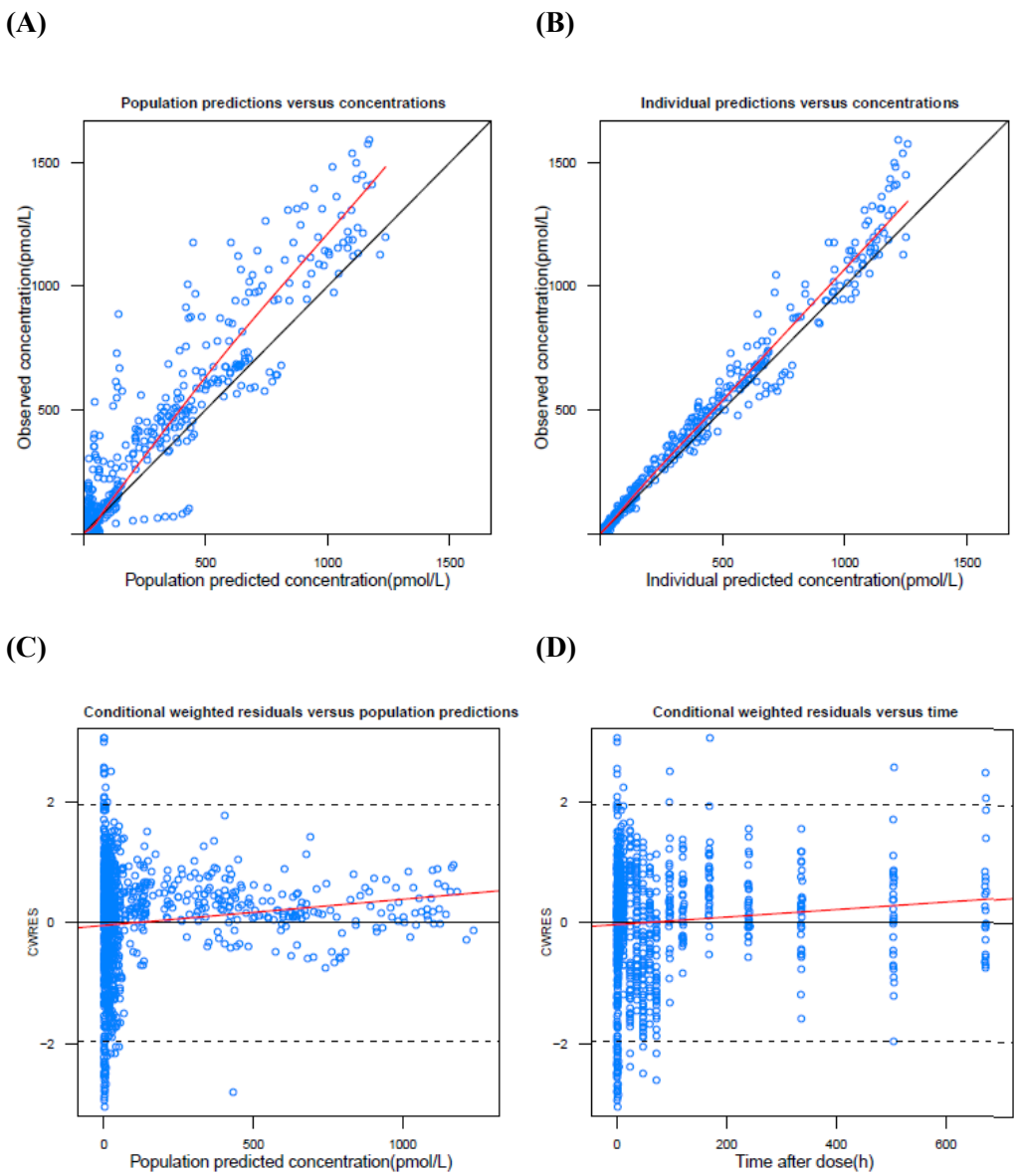

Figure 4. Goodness-of-fit plots for the final model (simple disposition model)
(A) Population predicted *versus* observed concentration, (B) Individual predicted *versus* observed concentration, (C) Population predicted concentration *versus* conditional weighted residual and (D) time *versus* conditional weighted residual. *Dots* represent observed data.
Abbreviations: CWRES, conditional weighted residuals

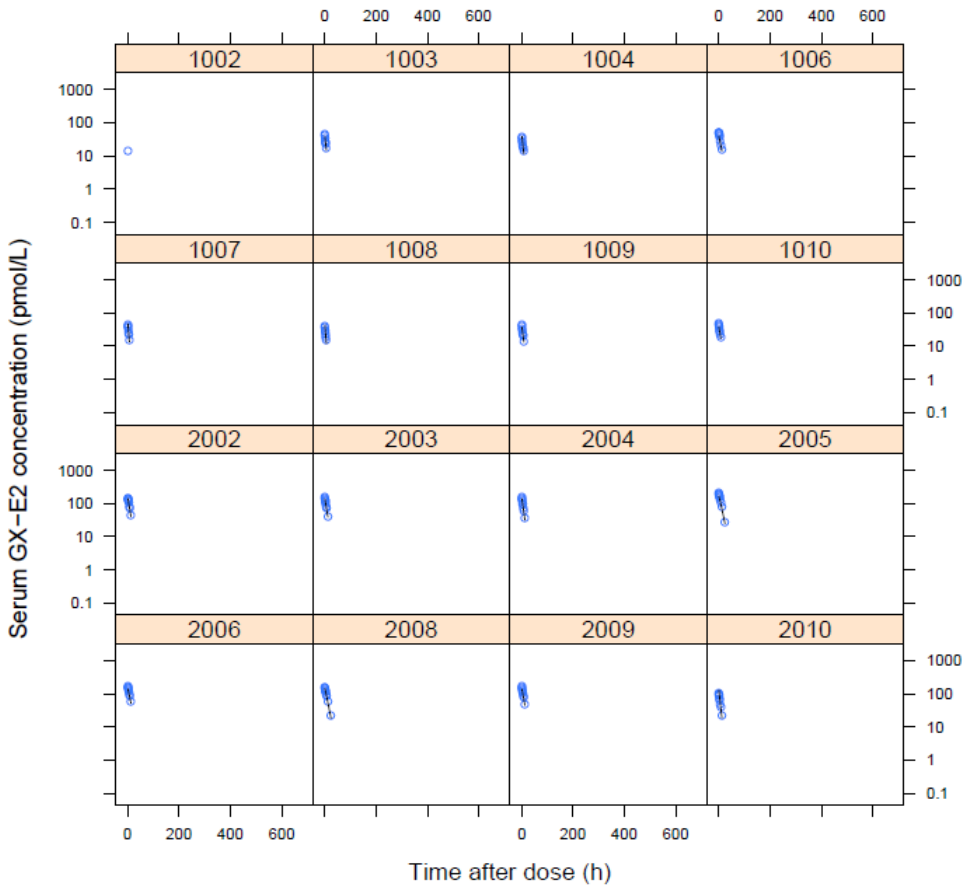

*Subject no. 1002, 1003, 1004, 1006, 1007, 1008, 1009 and 1010
: IV 0.3 μg/kg in study 1
*Subject no. 2002, 2003, 2004, 2005, 2006, 2008, 2009 and 2010
: IV 1 μg/kg in study 1

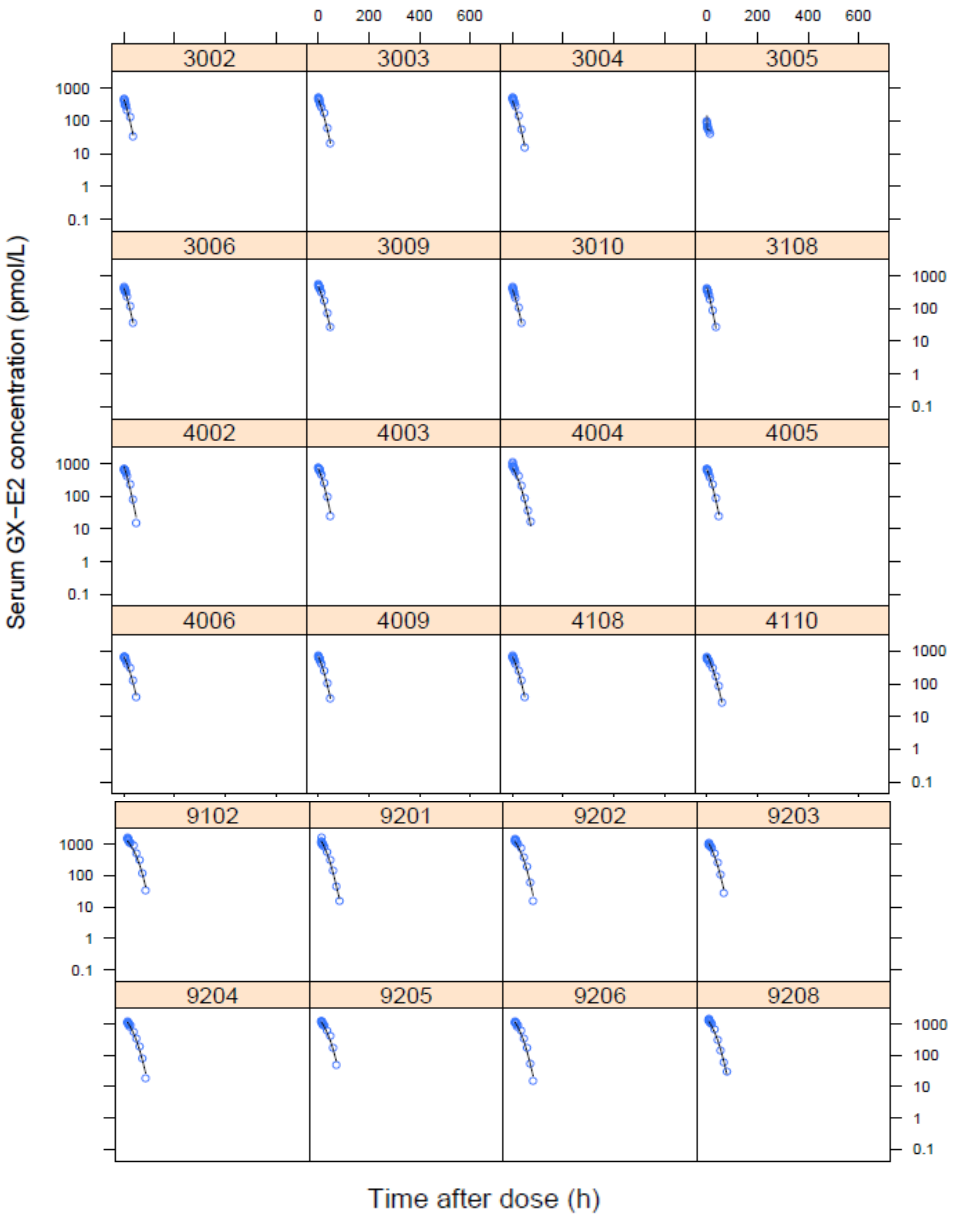

*Subject no. 3002, 3003, 3004, 3005, 3006, 3009, 3010 and 3018
: IV 3 μg/kg in study 1.
*Subject no. 4002, 4003, 4004, 4005, 4006, 4009, 4108 and 4110
: IV 5 μg/kg in study 1.
*Subject no. 8102, 8201, 8202, 8203, 8204, 8205, 8206 and 8208
: IV 5 μg/kg in study 2.

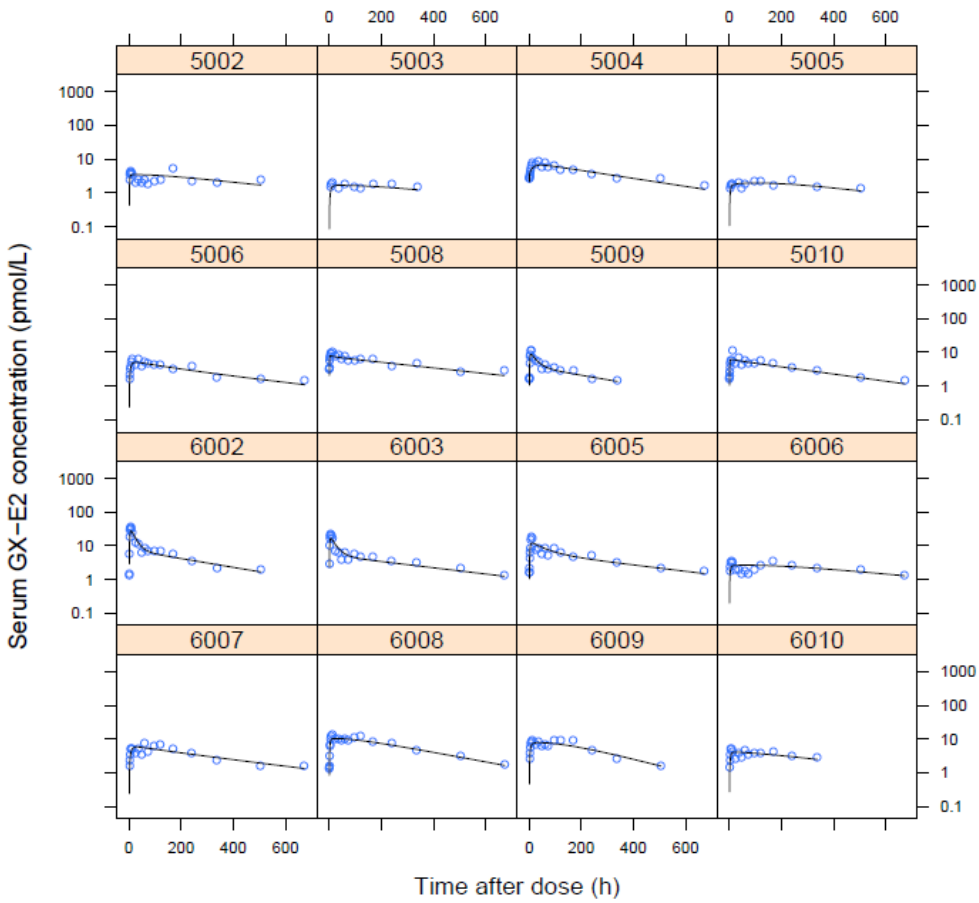

*Subject no. 5002, 5003, 5004, 5005, 5006, 5008, 5009 and 5010
: SC 0.3 μg/kg in study 1.
*Subject no. 6002, 6003, 6005, 6006, 6007, 6008, 6009 and 6010
: SC 1 μg/kg in study 1.

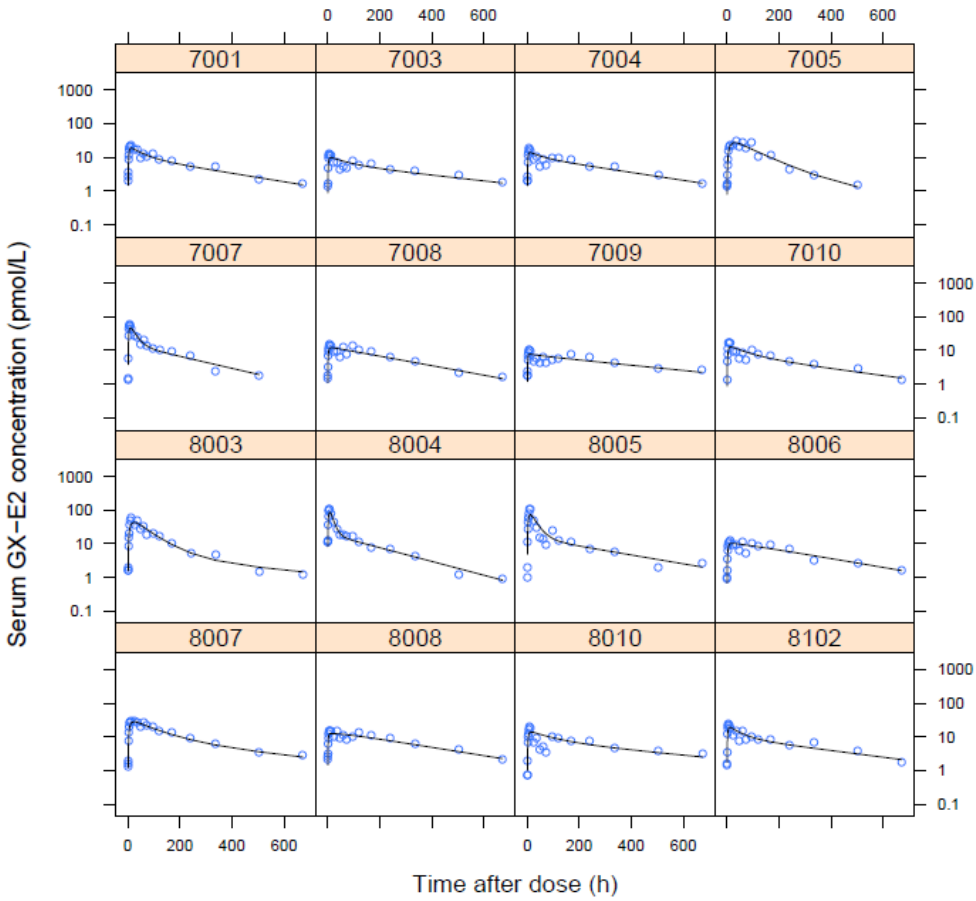

*Subject no. 7001, 7003, 7004, 7005, 7007, 7008, 7009 and 7010
: SC 3 μg/kg in study 1.
*Subject no. 8003, 8004, 8005, 8006, 8007, 8008, 8010 and 8102
: SC 5 μg/kg in study 1.

Figure 5. Individual serum GX-E2 concentration-time plots for the final simple disposition model (semi-logarithmic scale)

Dots represent observed concentration. *Solid lines* represent individual prediction.

Target-mediated disposition model

The two-compartment, target-on-tissue TMDD model also generally well characterized the PK profile of serum GX-E2. The OFV of the final TMDD model was 6005.485 and the AIC was 6292.55, which were both higher than the corresponding values of the final simple disposition model. Visual inspections for the covariate analysis did not present specific trend between IIV and potential covariates (Appendix 3). Hence, covariates were not included in the final TMDD model.

The estimated parameters of final TMDD model are presented in **Table 5**. The IIV were also allowed for all parameters except K_d, which was based on *in vitro* experimental results. Central and peripheral compartment volumes were estimated as 2.89 L and 1.26 L, respectively. The estimated volume of central compartment was comparable to that from the simple disposition model. CL_A and CL_B were 0.003 L/h and 5.4 L/h, indicating that injected GX-E2 mostly undergo the elimination as EPO-EPOR complex form. The proportional error was 31.7 %, which was also comparable to those of the simple disposition model. Regarding the absorption process, k_a and F value were estimated as 0.0003 h^{-1} and 0.766. While absorption rate constant was estimated with moderate IIV (45.2%), bioavailability presented relatively high IIV, exceeding 100%.

Figure 6 presents the goodness-of-fit plots for the TMDD models of intravenously injected GX-E2. The scatter plots of the observed *versus* population predicted concentrations and observed *versus* individual predicted concentrations were symmetrically distributed around the line of unity. The CWRES were randomly distributed around zero. No systematic bias in residuals was evident from the plots

of population predicted concentrations *versus* CWRES and time after dose *versus* CWRES. Besides, individual concentration-time plots indicated that most observations were adequately described by the TMDD model (**Figure 7**).

Table 5. Parameter estimates and inter-individual variability for the population PK model of GX-E2 (target-mediated disposition model)

Parameter	Definition	Population estimate (%RSE)	Inter-individual variability*
Pharmacokinetic parameter			
V_c (L)	Volume of central compartment	2.89 (13)	116.6
V_P (L)	Volume of peripheral compartment	1.26 (42)	180.8
Q (L/h)	Intercompartmental flow rate	1.3 (19)	126.9
CL_A (L/h)	Clearance of the free EPO	0.0003 (157)	29.4
CL_B (L/h)	Clearance of the EPO and EPO receptor complex	5.4 (36)	231.1
RB (pmol/L)	Input rate of EPO receptor	128 (7)	29.4
K_D (pmol/L)	Equilibrium association constant	200**	NA
k_a (h^{-1})	Absorption rate constant (first-order)	0.003 (22)	45.2
F	Bioavailability	0.766 (43)	116.2
Residual variability			
Proportional error (%)		31.7 (33)	-
Additional error (pmol/L)		0.001**	-
Running information			
Objective Function Value		6005.485	
Akaike Information Criteria		6292.546	
Elapsed estimation time (sec)		11432.60	

*Data is presented as percent (%).

**Fixed.

Abbreviations: RSE, relative standard error; EPO, erythropoietin.

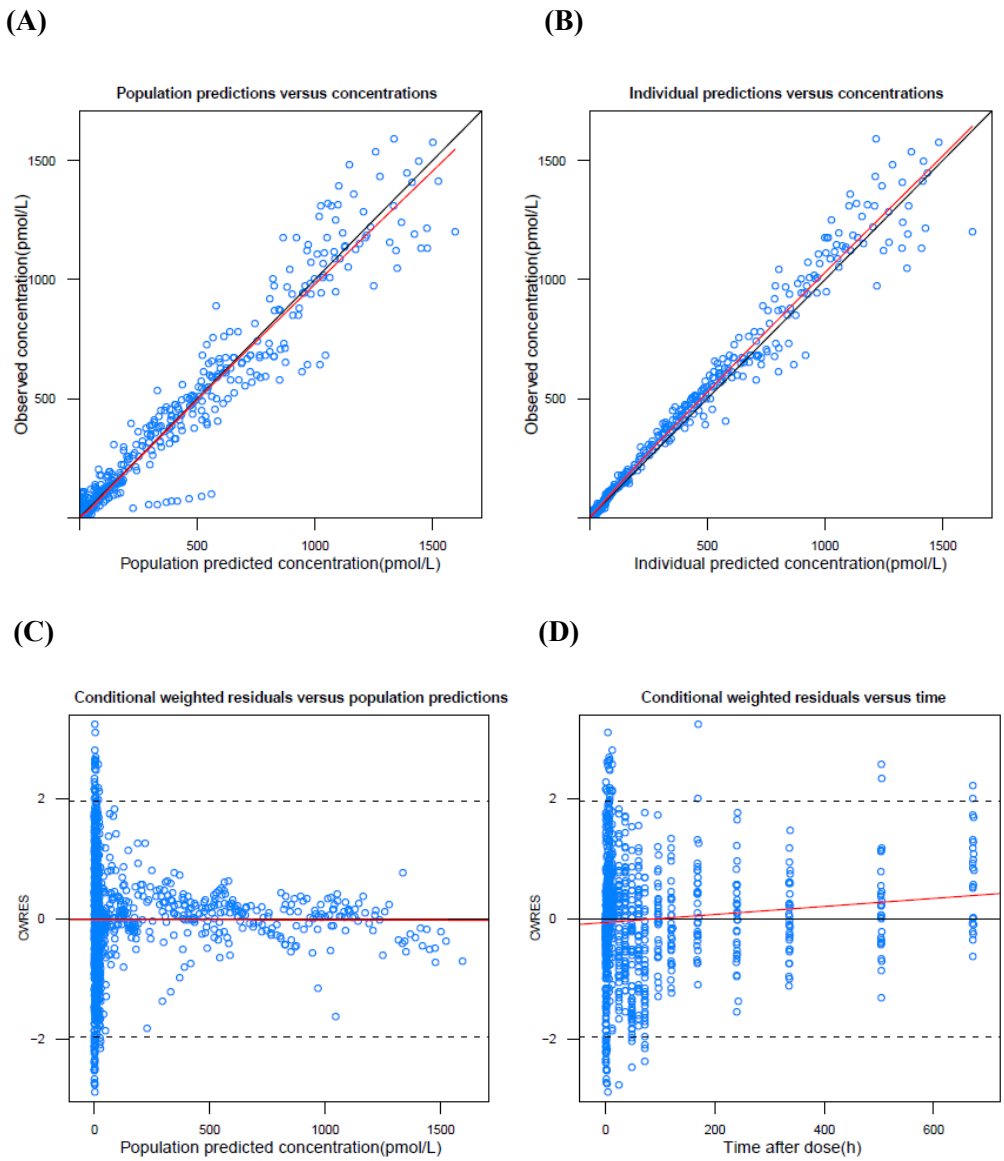

Figure 6. Goodness-of-fit plots for the final model (target mediated disposition model)

(A) Population predicted *versus* observed concentration, (B) Individual predicted *versus* observed concentration, (C) Population predicted concentration *versus* conditional weighted residual and (D) time *versus* conditional weighted residual. *Dots* represent observed data.

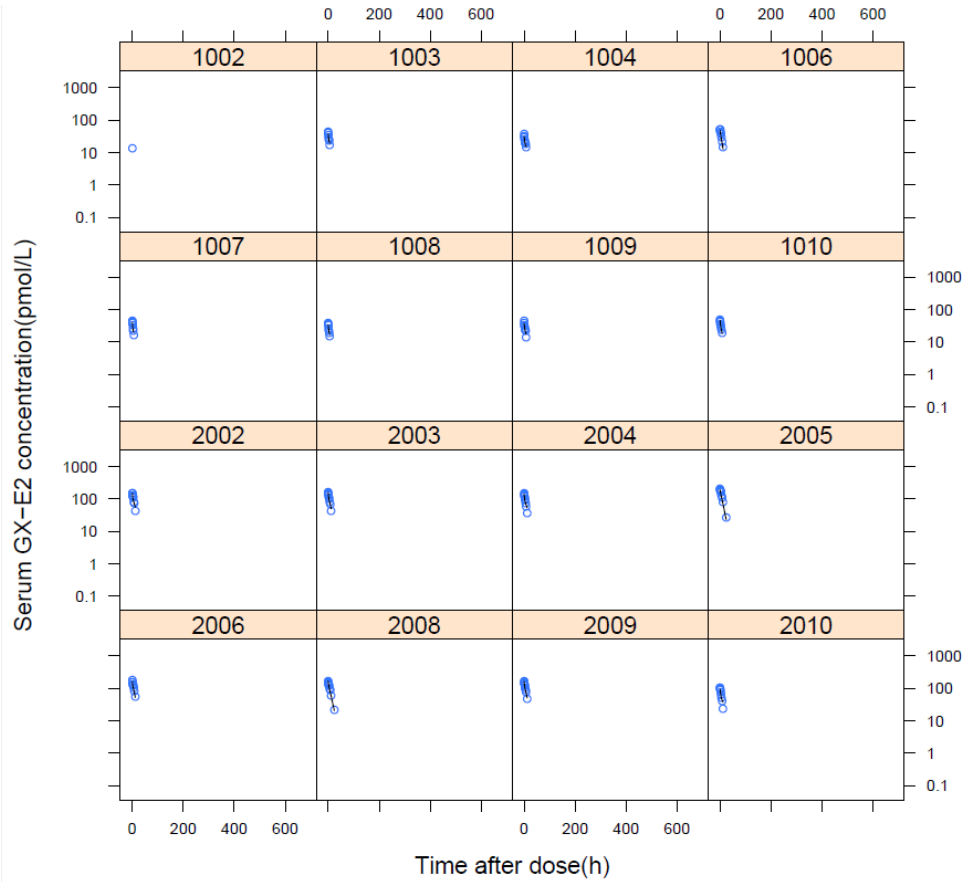

*Subject no. 1002, 1003, 1004, 1006, 1007, 1008, 1009 and 1010
: IV 0.3 μg/kg in study 1
*Subject no. 2002, 2003, 2004, 2005, 2006, 2008, 2009 and 2010
: IV 1 μg/kg in study 1

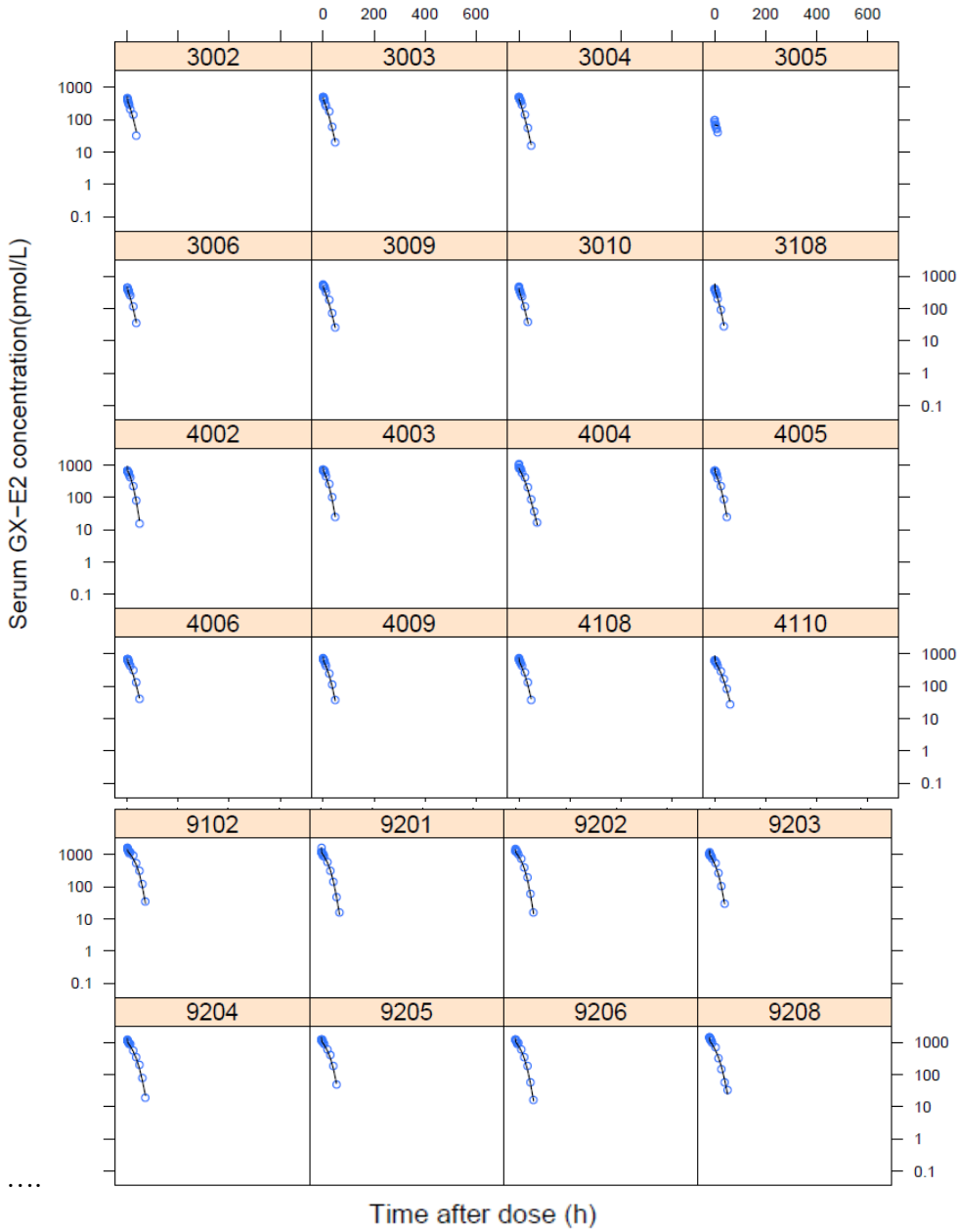

….

*Subject no. 3002, 3003, 3004, 3005, 3006, 3009, 3010 and 3018
: IV 3 μg/kg in study 1.
*Subject no. 4002, 4003, 4004, 4005, 4006, 4009, 4108 and 4110
: IV 5 μg/kg in study 1.
*Subject no. 8102, 8201, 8202, 8203, 8204, 8205, 8206 and 8208
: IV 5 μg/kg in study 2.

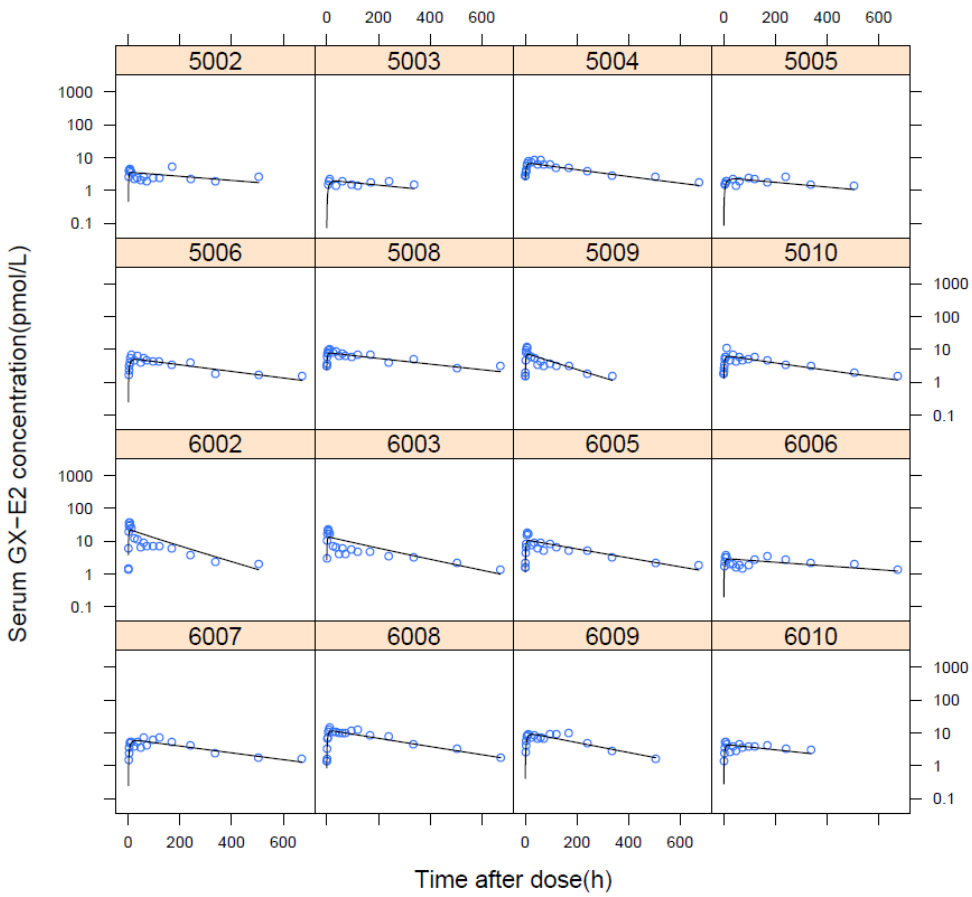

*Subject no. 5002, 5003, 5004, 5005, 5006, 5008, 5009 and 5010
: SC 0.3 μg/kg in study 1.
*Subject no. 6002, 6003, 6005, 6006, 6007, 6008, 6009 and 6010
: SC 1 μg/kg in study 1.

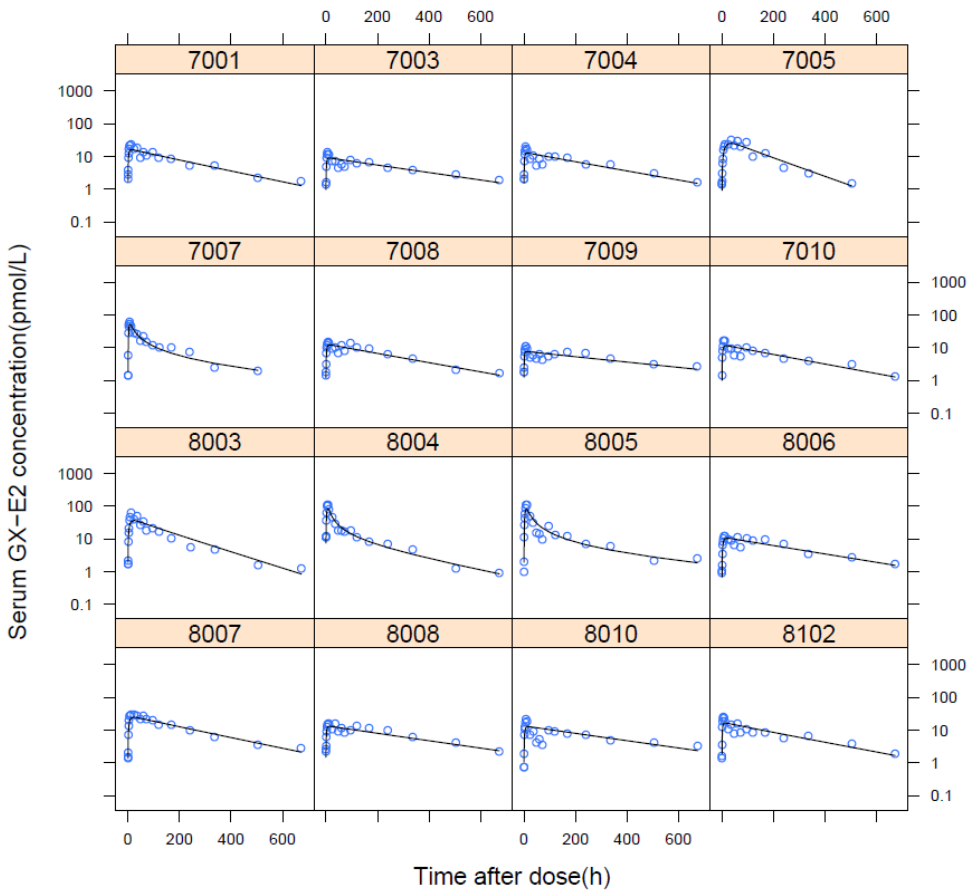

*Subject no. 7001, 7003, 7004, 7005, 7007, 7008, 7009 and 7010
: SC 3 μg/kg in study 1.
*Subject no. 8003, 8004, 8005, 8006, 8007, 8008, 8010 and 8102
: SC 5 μg/kg in study 1.

Figure 7. Individual serum GX-E2 concentration-time plots for the final simple disposition model (semi-logarithmic scale)

Dots represent observed data. *Solid lines* represent individual prediction.

Model validation

For the final simple disposition and TMDD models, pcVPC were performed to assess the predictive performance. The VPC results are shown by routes of administration in **Figure 8** and **Figure 9** for simple disposition model and TMDD model, respectively. The VPC plots indicate that the observed values (blue dots) and median (red solid line) with 5% and 95% percentiles (red dashed lines) are mostly within the 95% CIs (blue areas) of the 5^{th} and 95^{th} percentiles of the simulated values in both models. Accordingly, the final models were concluded to have adequate predictive performance.

(A) **(B)**

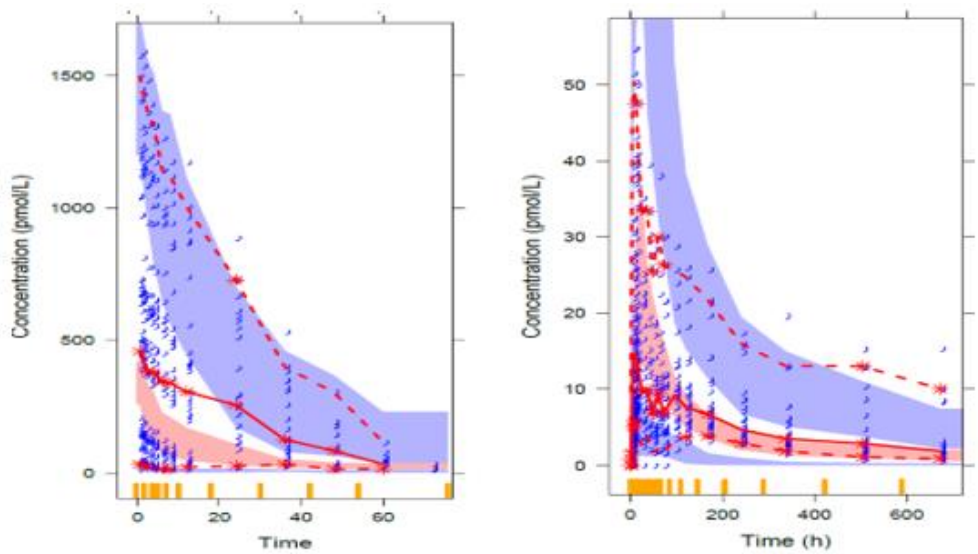

Figure 8. Prediction-corrected visual predictive check results stratified by route of administration
(simple disposition model)

(A) intravenous administration and (B) subcutaneous administration. *Solid line* represents median of observed data. *Dashed lines* represent 95% confidence interval of the observed data. *Blue shaded areas* represent 95% confidence interval around 5% and 95% percentiles of simulated values obtained by 1000 simulations. *Red shaded areas* represent 95% confidence interval around median of simulated values. *Circles* represent observed data.

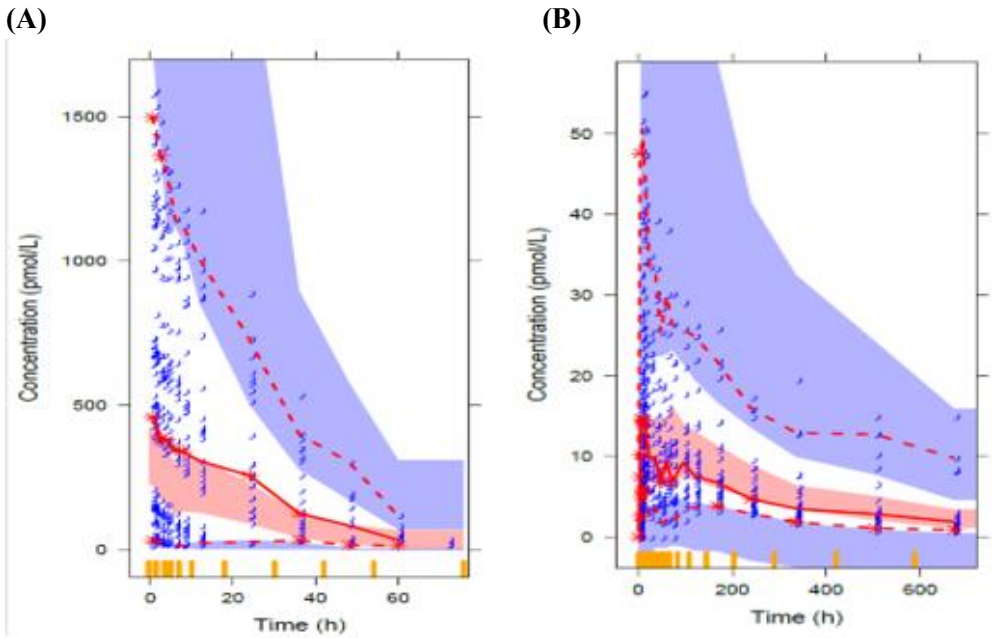

Figure 9. Prediction-corrected visual predictive check results stratified by route of administration
(target-mediated disposition model).

Left panel: intravenous administration, right panel: subcutaneous administration. *Solid line* represents median of observed data. *Dashed lines* represent 95% confidence interval of the observed data. *Blue shaded areas* represent 95% confidence interval around 5% and 95% percentiles of simulated values obtained by 1000 simulations. *Red shaded areas* represent 95% confidence interval around median of simulated values. *Circles* represent observed data.

DISCUSSION

GX-E2 is a newly developed erythropoiesis stimulating agent that incorporates continuous protein antibody fusion technology. Thus far, two phase I clinical trials that assessed the PK properties of GX-E2 in healthy male volunteers have been conducted. The present work tried to stretch the PK characterization of GX-E2 by developing population PK models using the nonlinear mixed effect approach.

In prior to the population PK modeling, explanatory data analysis was conducted. As observed with other rhuEPO, non-linear disposition was presented after the IV injection of GX-E2. Following SC injection of GX-E2, slow absorption process was observed, leading to maximal concentration at 6 to 240-hour post-dose. To incorporate the explored PK properties of GX-E2 within the population PK model, two different approaches were employed: simple disposition model explaining non-linear properties with saturable elimination pathway parameterized by V_m and K_m and mechanistic TMDD model which reflect the binding of drug on receptor and receptor-mediated endocytosis process. Absorption was described as the first-order process in both models.

Both final simple disposition model and TMDD model were fitted with the observed data well. The final simple disposition model was comprised of two compartments with Michaelis-Menten parameters, V_m and K_m. This model had advantages of relatively simple model structure with fewer parameters and shorter elapsed time when compared with the TMDD model. As in this work, Michaelis-Menten models have been successfully described the PK characteristics of target-

binding drugs presenting non-linear disposition. However, Michaelis-Menten models could not reflect target binding and receptor-mediated endocytosis within models, which are attributable to non-linear disposition. For instance, Michaelis-Menten model will not be able to capture the characteristic PK properties of antibody drugs such as initial decay of the drug concentration due to the rapid drug-target binding. (22) In this study, binding of EPO and its receptor is usually proceeded very rapidly (less than 5 minutes), and PK sampling interval may not be adequate to capture this process. (22, 34)

Although the TMDD model has rather complex base structure, it provides information about underlying molecular events of EPO and its target receptor such as the binding of EPO and EPOR, internalization of EPO-EPOR complex, and EPO receptor turnover. (19) Furthermore, the TMDD model enables to assess the drug concentrations under free and bound form.

From the TMDD model, the clearance of bound GX-E2 (CL_B) was estimated as 5.4 L/h while unbound GX-E2 clearance (CL_A) was 0.0003 L/h, indicating that majority of injected GX-E2 is eliminated in the bound form. The RB, the input rate (production rate) of EPO receptor was estimated as 127 pmol/h, which was consistent with other reported EPO receptor input rate value. (21, 31)

Both models described the absorption process as a single-pathway, first-order process. When compared with darbepoetin alfa PK model with first-order absorption process, estimated value for k_a was relatively low (0.003 – 0.01 h^{-1} and 0.0212 h^{-1} for GX-E2 and darbepoetin alfa, respectively). Due to their large molecular size, therapeutic proteins are mainly absorbed into the lymphatic system before absorbed into the systemic circulation via blood capillaries. (40) As the lymphatic flow is

slow (approximately 120 mL/day in human), therapeutic proteins are slowly distributed from injected site to systemic circulation. (19) Considering that molecular weights of darbepoetin alfa and GX-E2 is 38.4 kDa and 120 kDa, respectively, the slower absorption of GX-E2 is reasonable.

The VPC were performed to validate the predictive performance of each model. The results indicated that the simulation results from both models generally well reflected the observed data. In the simple disposition model, less than 10 observed data deviated from the 95% CI of the 95th percentiles of the simulation. In addition, 95% CI of the observed data after 400 hours following the SC injection were over the 95% CI of the 95th percentile from the simulation, indicating the simple disposition model may underestimate the serum drug concentrations (**Figure 8**). More variabilities were observed in the TMDD model when compared to those of the single disposition model. However, all observed data with 5%-95% CI located within shaded area in the TMDD model (**Figure 9**).

There are a few limitations in this work to address. First, dual peaks were observed within most subjects in SC administered groups. In the current model, only a single absorption pathway was taken into account for the model simplicity and thereby could not capture the second absorption peak. Introduction of the dual absorption pathway including lymphatic pathway will enable to capture the second peak and ultimately improve the model fit. (15, 41) Furthermore, PD components were not considered. The PK properties of rhuEPO are affected by PD components. For instance, downregulation of EPO receptor production is caused by intracellular signaling from the binding of EPO and EPOR. In addition, circulating red blood

cell leads the negative feedback control of EPO production. (13, 42) When the current TMDD PK model is linked with PD model incorporating PK-PD interplay, the mechanism-based quantitative assessment of exposure-response relationship in GX-E2 can be achieved. Ultimately, the obtained results from the modeling and simulation could be utilized as a rationale for optimizing dosing regimen.

To conclude, the present work is the first to propose the population PK model following a single IV or SC injection of GX-E2. Both two compartment with Michaelis-Menten enzyme kinetic model (simple disposition model) and target-on-tissue TMDD model successfully fitted with the observed clinical data. Slow absorption profiles were explained with first-order absorption constant. When the proposed model in this study is supplemented by PD data, it is expected to have a role in suggesting future dosing regimens.

ACKNOWLEDMENTS

This study was supported by the Genexine, Inc., Green Cross Corp., and Ministry of Health & Welfare, Republic of Korea.

REFERENCES

1. Tsagalis G. Renal anemia: a nephrologist's view. Hippokratia. 2011;15(Suppl 1):39-43.
2. Kidney Disease Improving Global Outcomes (KDIGO) Anemia Work Group. KDIGO Clinical Practice Guideline for Anemia in Chronic Kidney Disease. Kidney inter, Suppl. 2012;2:279–335.
3. Im SJ, Yang SI, Yang SH, Choi DH, Choi SY, Kim HS, et al. Natural form of noncytolytic flexible human Fc as a long-acting carrier of agonistic ligand, erythropoietin. PLoS One. 2011;6(9):e24574.
4. Rath T, Baker K, Dumont JA, Peters RT, Jiang H, Qiao SW, et al. Fc-fusion proteins and FcRn: structural insights for longer-lasting and more effective therapeutics. Crit Rev Biotechnol. 2015;35(2):235-54.
5. Powell JS, Josephson NC, Quon D, Ragni MV, Cheng G, Li E, et al. Safety and prolonged activity of recombinant factor VIII Fc fusion protein in hemophilia A patients. Blood. 2012;119(13):3031-7.
6. Shapiro AD, Ragni MV, Valentino LA, Key NS, Josephson NC, Powell JS, et al. Recombinant factor IX-Fc fusion protein (rFIXFc) demonstrates safety and prolonged activity in a phase 1/2a study in hemophilia B patients. Blood. 2012;119(3):666-72.
7. Han H, Lee J, Shin D, Shin KH, Jeon H, Lim KS, et al. Pharmacodynamics, pharmacokinetics, and tolerability of intravenous or subcutaneous GC1113, a novel erythropoiesis-stimulating agent. Clin Drug Investig. 2014;34(6):373-82.
8. Grady J, Linet O. Early Phase Drug Evaluation in Man. Boca Raton, FL, USA: CRC Press, Inc; 1990.
9. Sheiner LB, Rosenberg B, Melmon KL. Modelling of individual pharmacokinetics for computer-aided drug dosage. Comput Biomed Res. 1972;5(5):411-59.
10. Sheiner LB, Rosenberg B, Marathe VV. Estimation of population characteristics of pharmacokinetic parameters from routine clinical data. J Pharmacokinet Biopharm. 1977;5(5):445-79.
11. Sun H, Fadiran EO, Jones CD, Lesko L, Huang SM, Higgins K, et al. Population pharmacokinetics. A regulatory perspective. Clin Pharmacokinet. 1999;37(1):41-58.
12. U.S. Department of Health and Human Services FaDA, Center for Drug Evaluation and Research (CDER) and Center for Biologics Evaluation and Research (CBER);. Guidance for Industry: Population Pharmacokinetics. 1999.
13. Yan X, Lowe PJ, Fink M, Berghout A, Balser S, Krzyzanski W. Population pharmacokinetic and pharmacodynamic model-based comparability assessment of a recombinant human Epoetin Alfa and the Biosimilar HX575. J Clin Pharmacol. 2012;52(11):1624-44.
14. Agoram B, Heatherington AC, Gastonguay MR. Development and evaluation of a population pharmacokinetic-pharmacodynamic model of darbepoetin alfa in patients with nonmyeloid malignancies undergoing multicycle

chemotherapy. AAPS J. 2006;8(3):E552-63.
15. Olsson-Gisleskog P, Jacqmin P, Perez-Ruixo JJ. Population pharmacokinetics meta-analysis of recombinant human erythropoietin in healthy subjects. Clin Pharmacokinet. 2007;46(2):159-73.
16. Hayashi N, Kinoshita H, Yukawa E, Higuchi S. Pharmacokinetic analysis of subcutaneous erythropoietin administration with nonlinear mixed effect model including endogenous production. British journal of clinical pharmacology. 1998;46(1):11-9.
17. Ramakrishnan R, Cheung WK, Wacholtz MC, Minton N, Jusko WJ. Pharmacokinetic and pharmacodynamic modeling of recombinant human erythropoietin after single and multiple doses in healthy volunteers. J Clin Pharmacol. 2004;44(9):991-1002.
18. Veng-Pedersen P, Widness JA, Pereira LM, Peters C, Schmidt RL, Lowe LS. Kinetic evaluation of nonlinear drug elimination by a disposition decomposition analysis. Application to the analysis of the nonlinear elimination kinetics of erythropoietin in adult humans. Journal of pharmaceutical sciences. 1995;84(6):760-7.
19. Dostalek M, Gardner I, Gurbaxani BM, Rose RH, Chetty M. Pharmacokinetics, pharmacodynamics and physiologically-based pharmacokinetic modelling of monoclonal antibodies. Clin Pharmacokinet. 2013;52(2):83-124.
20. Mager DE. Target-mediated drug disposition and dynamics. Biochem Pharmacol. 2006;72(1):1-10.
21. Krzyzanski W, Wyska E. Pharmacokinetics and pharmacodynamics of erythropoietin receptor in healthy volunteers. Naunyn Schmiedebergs Arch Pharmacol. 2008;377(4-6):637-45.
22. Yan X, Mager DE, Krzyzanski W. Selection between Michaelis-Menten and target-mediated drug disposition pharmacokinetic models. J Pharmacokinet Pharmacodyn. 2010;37(1):25-47.
23. ICH Harmonised Tripartite Guideline: guideline for good clinical practice. J Postgrad Med. 2001;47(2):121-30.
24. General Assembly of the World Medical A. World Medical Association Declaration of Helsinki: ethical principles for medical research involving human subjects. J Am Coll Dent. 2014;81(3):14-8.
25. Keizer RJ, Karlsson MO, Hooker A. Modeling and Simulation Workbench for NONMEM: Tutorial on Pirana, PsN, and Xpose. CPT Pharmacometrics Syst Pharmacol. 2013;2:e50.
26. Wang Y. Derivation of various NONMEM estimation methods. J Pharmacokinet Pharmacodyn. 2007;34(5):575-93.
27. Beal SL, Sheiner LB, Boeckmann A, Bauer RJ. NONMEM Users Guide. Hanover, MD.: ICON Development Solutions.; 2014.
28. Karlsson KE, Plan EL, Karlsson MO. Performance of three estimation methods in repeated time-to-event modeling. AAPS J. 2011;13(1):83-91.
29. Yun H, CHae J, Kwon K. Comparison of Estimation Methods in NONMEM 7.2: Application to a Real Clinical Trial Dataset. Korean Journal of Clinical Pharmacy. 2013;23(2):137-41.
30. Sheiner LB, Beal SL. Evaluation of methods for estimating population pharmacokinetics parameters. I. Michaelis-Menten model: routine clinical

pharmacokinetic data. J Pharmacokinet Biopharm. 1980;8(6):553-71.
31. Woo S, Krzyzanski W, Jusko WJ. Target-mediated pharmacokinetic and pharmacodynamic model of recombinant human erythropoietin (rHuEPO). J Pharmacokinet Pharmacodyn. 2007;34(6):849-68.
32. Mould DR, Upton RN. Basic concepts in population modeling, simulation, and model-based drug development-part 2: introduction to pharmacokinetic modeling methods. CPT Pharmacometrics Syst Pharmacol. 2013;2:e38.
33. Mager DE, Jusko WJ. General pharmacokinetic model for drugs exhibiting target-mediated drug disposition. J Pharmacokinet Pharmacodyn. 2001;28(6):507-32.
34. Gross AW, Lodish HF. Cellular trafficking and degradation of erythropoietin and novel erythropoiesis stimulating protein (NESP). J Biol Chem. 2006;281(4):2024-32.
35. Lowe PJ, Tannenbaum S, Wu K, Lloyd P, Sims J. On setting the first dose in man: quantitating biotherapeutic drug-target binding through pharmacokinetic and pharmacodynamic models. Basic Clin Pharmacol Toxicol. 2010;106(3):195-209.
36. Gibiansky L, Gibiansky E. Target-mediated drug disposition model: approximations, identifiability of model parameters and applications to the population pharmacokinetic-pharmacodynamic modeling of biologics. Expert Opin Drug Metab Toxicol. 2009;5(7):803-12.
37. Wilks SS. The Large-Sample Distribution of the Likelihood Ratio for Testing Composite Hypotheses. The Annals of Mathematical Statistics.9(1):60-2.
38. Holford N. The visual predictive check—superiority to standard diagnostic (Rorschach) plots. .PAGE 14 (2005) Abstr 738 [www.page-meeting.org/?abstract=738].
39. Bergstrand M, Hooker AC, Wallin JE, Karlsson MO. Prediction-corrected visual predictive checks for diagnosing nonlinear mixed-effects models. AAPS J. 2011;13(2):143-51.
40. Supersaxo A, Hein WR, Steffen H. Effect of molecular weight on the lymphatic absorption of water-soluble compounds following subcutaneous administration. Pharm Res. 1990;7(2):167-9.
41. Kagan L. Pharmacokinetic modeling of the subcutaneous absorption of therapeutic proteins. Drug Metab Dispos. 2014;42(11):1890-905.
42. Wang YM, Krzyzanski W, Doshi S, Xiao JJ, Perez-Ruixo JJ, Chow AT. Pharmacodynamics-mediated drug disposition (PDMDD) and precursor pool lifespan model for single dose of romiplostim in healthy subjects. AAPS J. 2010;12(4):729-40.

APPENDICES

Appendix 1. Summary of the pharmacokinetic parameters after a single intravenous or sub-cutaneous administration of GX-E2 (non-compartmental analysis)

Appendix 2. Scatter plots for IIV of parameter *versus* covariates (simple disposition model)

Appendix 3. Scatter plots for IIV of parameter *versus* covariates (TMDD model)

Appendix 1. Summary of the pharmacokinetic parameters after a single intravenous or subcutaneous administration of GX-E2 (non-compartmental analysis)

	Study								
	1				2				
Dose	**0.3 μg/kg IV**	**1 μg/kg IV**	**3 μg/kg IV**	**5 μg/kg IV**	**1 μg/kg SC**	**3 μg/kg SC**	**5 μg/kg SC**	**8 μg/kg SC**	**8 μg/kg IV**
Number of subjects	8	8	8	8	8	8	8	8	8
T_{max} (h)	-	-	-	-	12 [6-240.35]	8.02 [6-168.53]	6 [6-36]	36 [8-36.02]	0.75 [0.25-1]
C_{max} (μg/L)	4.82 (1.40)	18.99 (3.47)	51.41 (16.80)	88.09 (15.53)	0.87 (0.45)	1.72 (1.26)	2.81 (1.88)	5.71 (4.80)	162.53 (22.68)
AUC_{last} (h·μg/L)	21.32 (12.07)	147.61 (57.76)	826.32 (342.03)	1759.65 (315.09)	198.46 (106.27)	287.46 (102.65)	443.24 (73.23)	615.97 (147.05)	4033.20 (677.55)
$AUC_{0\text{-}24h}$ (h·μg/L)	37.39 (9.52)	173.14 (49.14)	694.11 (251.92)	1325.33 (168.77)	13.98 (8.17)	27.47 (19.43)	46.81 (29.3)	95.51 (77.23)	2643.21 (13.35)
AUC_{inf} (h·μg/L)	39.82 (10.78)	191.33 (59.51)	877.60 (323.03)	1799.65 (313.28)	341.74 (179.32)	374.97 (83.07)	514.52 (54.12)	716.07 (136.88)	4068.62 (696.17)
CL/F (L/h/kg)	0.008 (0.002)	0.006 (0.002)	0.005 (0.005)	0.003 (0.000)	3.67 (1.71)	8.30 (1.61)	9.81 (1.04)	11.57 (2.41)	0.002 (0.0003)
MRT (h)	1.99 (0.89)	3.87 (1.02)	7.98 (1.92)	10.51 (1.34)	227.83 (47.81)	218.73 (51.65)	210.52 (53.82)	199.78 (52.57)	22.29 (2.58)

Data are presented as the mean (standard deviation).

*Data are presented as median [minimum – maximum].

Abbreviations: IV, intravenous; SC, subcutaneous; C_{max}, maximum observed concentration; AUC_{last}, area under the curve from the time of dosing to the last measurable concentration; $AUC_{0\text{-}24h,}$ area under the curve from the time of dosing to the 24-hour post-dose. AUC_{inf}, area under the curve from the time of dosing extrapolated to infinity, based on the last observed concentration; CL/F, apparent total body clearance; MRT, mean residence time.

Appendix 2. Scatter plots for IIV of parameter *versus* covariates (simple disposition model)

IIV on V_C | **IIV on Q**

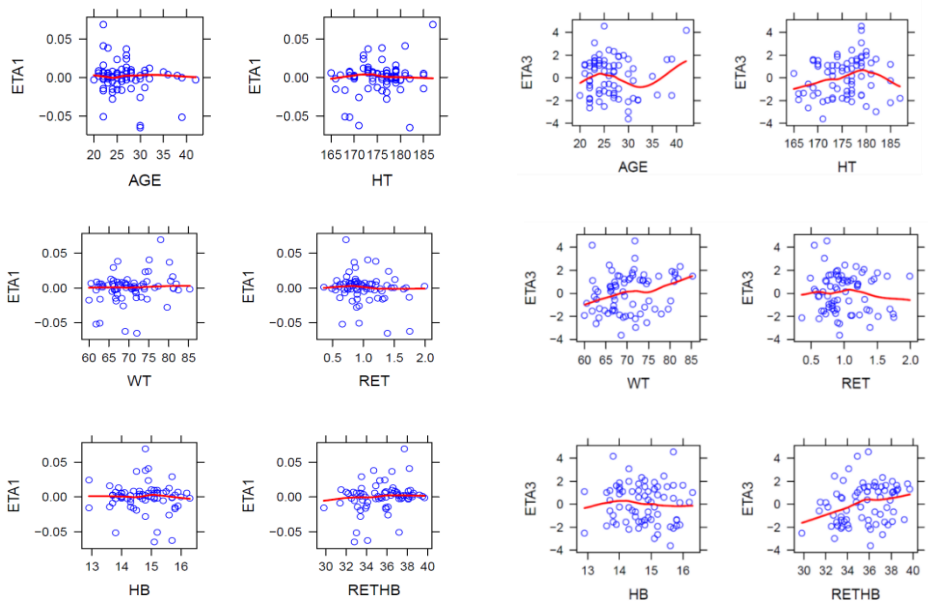

IIV on V_P | **IIV on K_m**

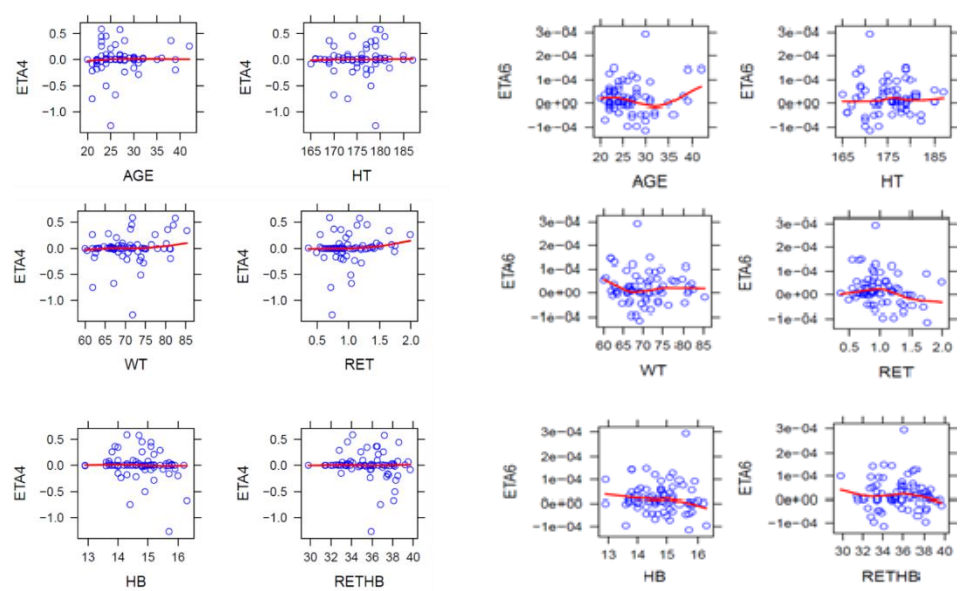

Appendix 3. Scatter plots for IIV of parameter *versus* covariates (TMDD model)

IIV on CL_A

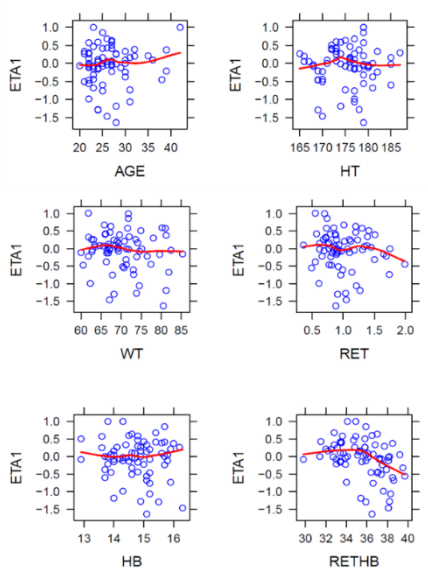

IIV on V_C

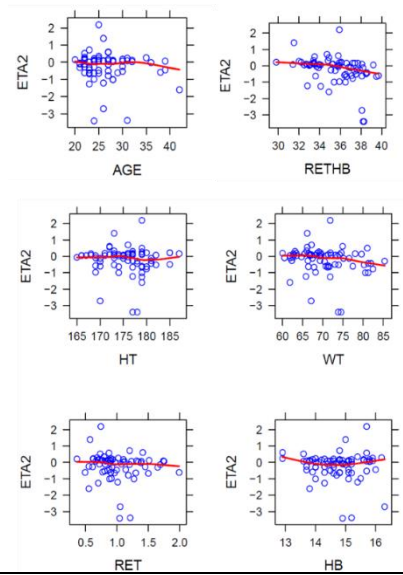

IIV on Q

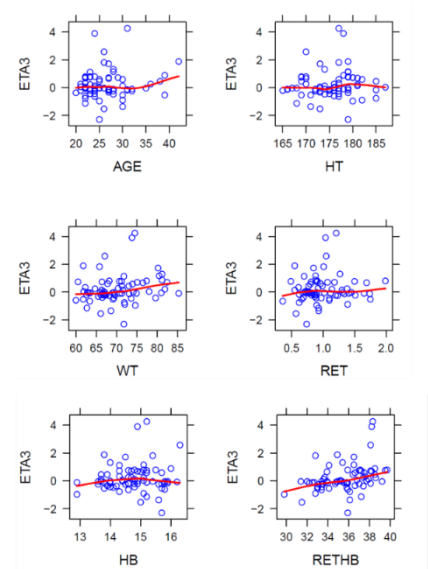

IIV on RB

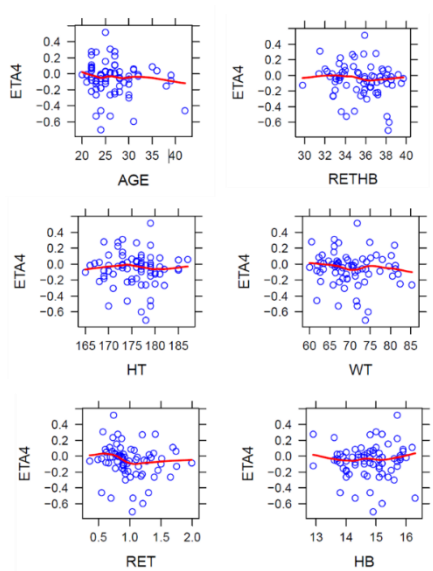

(continued)

IIV on CL_B	IIV on V_P

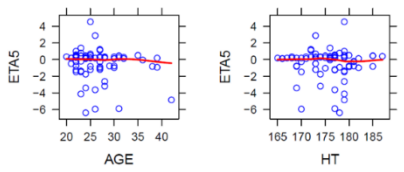

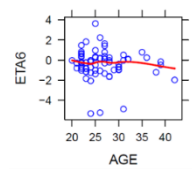

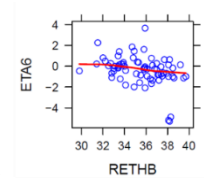

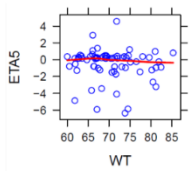

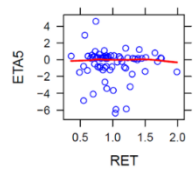

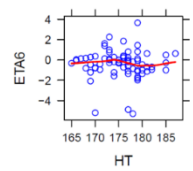

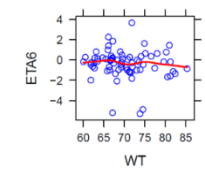

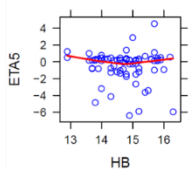

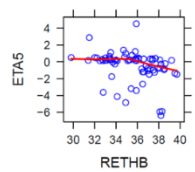

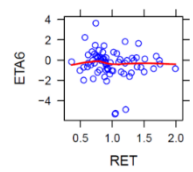

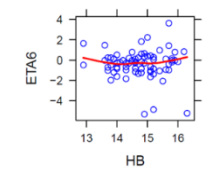

국문 초록

새로운 적혈구 생성 촉진제인 GX-E2 의 집단 약동학 분석

서론: GX-E2는 에리스로포이에틴(EPO)에 항체의 Fc 영역 혼성체를 결합한 새로운 기전의 적혈구 생성 촉진제이다. 비임상 및 임상시험 데이터를 비구획 분석하여 GX-E2를 단회 정맥 및 피하 주사 시 약동 · 약력학적 특성을 확인하였으며, 피하 주사 시 시판 중인 EPO 제제에 비하여 긴 체내 잔류 시간 및 작용 시간을 나타냄을 확인하였다. 본 연구에서는 건강 자원자에게 GX-E2를 정맥 및 피하 주사 시 약동학 양상을 정량적으로 확인하고자 집단약동학 모델을 개발하였다.

방법: 모델 개발을 위하여 2건의 1상 임상시험 데이터를 수집하였다. 약물의 제거 양상을 기술하기 위하여 두 가지 접근법으로 각각의 모델을 개발하였다. 단순 배치 모델(simple disposition model)에서는 Michaelis-Menten enzyme kinetics을 활용하였으며 약동학을 기전적으로 설명하기 위하여 수용체 매개 약물 배치(target-mediated drug disposition)모델도 개발하였다. 적합도 플롯 및 목적함수값을 기반으로 각 모델을 평가하여 최종 모델을

선정하였으며 최종 모델의 예측력은 시각적 예측 확인(visual predictive check)으로 검증하였다.

결과: 총 72명의 대상자로부터 1084개의 혈청 EPO 농도를 수집하였다. GX-E2의 약동학은 2구획, 1차 흡수 모델로 적절히 설명가능하였다. 단순 배치 모델 및 TMDD 모델 모두 관측값을 적절히 적합하였다. 시각적 예측 확인을 통하여 각 최종 모델의 예측력을 확인하였다. 피하 주사 시 약 50-70% 가 0.003 h^{-1} 의 흡수 상수로 느리게 전신 흡수되는 것으로 예측되었다. 또한 TMDD 모델에서 예측한 결합 및 비결합 청소율을 통하여 주입된 GX-E2는 대부분 결합형으로 제거됨을 알 수 있었다.

결론: 단순 배치 및 TMDD 모델 모두 정맥 · 피하 주사 후 GX-E2의 약동학을 적절히 예측하였으나 TMDD 모델은 약물의 기전을 반영한다는 이점을 갖고 있다. 현 모델에 기전적 특성을 반영한 흡수 및 약력학 요소를 포함할 시 GX-E2의 약동학 양상을 보다 심도있게 이해할 수 있을 것이다.

주요어: 집단 약동학; 비선형혼합효과모델링(NONMEM); 에리스로포이에틴; GX-E2; 적혈구 생성 촉진제

학 번: 2015-23241